



## Article

# Changing Carboniferous Arc Magmatism in the Ossa-Morena Zone (Southwest Iberia): Implications for the Variscan Belt

Manuel Francisco Pereira <sup>1,\*</sup>, José Manuel Fuenlabrada <sup>2</sup> , Carmen Rodríguez <sup>3</sup>  and António Castro <sup>3</sup>

<sup>1</sup> Departamento de Geociências, Instituto de Ciências da Terra, ECT, Universidade de Évora, Apt. 94, 7002-554 Evora, Portugal

<sup>2</sup> Unidad de Geocronología (CAI de Ciencias de la Tierra y Arqueometría), Universidad Complutense de Madrid, 28040 Madrid, Spain; jmfuenla@pdi.ucm.es

<sup>3</sup> Instituto Andaluz de Ciencias de la Tierra (IACT), Consejo Superior de Investigaciones Científicas-Universidad de Granada, 18100 Armilla, Spain; carmenrdealmodovar@gmail.com (C.R.); antonio.castro@csic.es (A.C.)

\* Correspondence: mpereira@uevora.pt

**Abstract:** Carboniferous magmatism in southwestern Iberia was continuously active for more than 60 m.y. during the development of the Appalachian-Variscan belt of North America, North Africa and Western-Central Europe. This collisional orogen that records the closure of the Rheic Ocean is essential to understanding the late Paleozoic amalgamation of the Pangea supercontinent. However, the oblique convergence between Laurussia and Gondwana that lasted from the Devonian to the Carboniferous was likely more complex. Recently, a new tectonic model has regarded the Iberia Variscan belt as the site of coeval collisional and accretionary orogenic processes. Early Carboniferous plutonic rocks of southwest Iberia indicate arc magmatism in Gondwana. The Ossa-Morena Zone (OMZ) acted as the upper plate in relation to the geometry of the Paleotethys subduction. This active accretionary-extensional margin was progressively involved in a collisional phase during the Late Carboniferous. Together, the Évora Massif and the Beja Igneous Complex include three successive stages of bimodal magmatism, with a chemical composition indicative of a long-lived subduction process lasting from the Tournaisian to the Moscovian in the OMZ. The earliest stage of arc magmatism includes the Tournaisian Beja and Torrão gabbro-dioritic rocks of the Layered Gabbroic Sequence. We present new geochemical and Nd isotopic and U-Pb geochronological data for magmatic rocks from the Main (Visean-Serpukhovian) and Latest (Bashkirian-Moscovian) stages of arc magmatism. Visean Toca da Moura trachyandesite and rhyolites and Bashkirian Baleizão porphyries and Alcáçovas quartz diorite share enriched, continental-crust like characteristics, as indicated by major and trace elements, mainly suggesting the addition of calc-alkaline magma extracted from various mantle sources in a subduction-related setting (i.e., Paleotethys subduction). New U-Pb zircon geochronology data have allowed us to establish a crystallization age of  $317 \pm 3$  Ma (Bashkirian) for Alcáçovas quartz diorite that confirms a temporal link with Baleizão porphyry. Positive  $\epsilon\text{Nd}(t)$  values for the Carboniferous igneous rocks of the Beja Igneous Complex and the Évora gneiss dome indicate production of new juvenile crust, whereas negative  $\epsilon\text{Nd}(t)$  values also suggest different grades of magma evolution involving crustal contamination. The production and evolution of Carboniferous continental crust in the OMZ was most likely associated with the development of an active continental margin during the convergence of the Paleotethys Ocean with Gondwana, involving juvenile materials and different grades of crustal contamination.

**Keywords:** arc magmatism; Variscan belt; wr-geochemistry; Sm-Nd isotopes; U-Pb geochronology; Paleotethys margin



**Citation:** Pereira, M.F.; Fuenlabrada, J.M.; Rodríguez, C.; Castro, A. Changing Carboniferous Arc Magmatism in the Ossa-Morena Zone (Southwest Iberia): Implications for the Variscan Belt. *Minerals* **2022**, *12*, 597. <https://doi.org/10.3390/min12050597>

Academic Editors: Antonios Koroneos, Ioannis Baziotis and Kristina Šarić

Received: 31 March 2022

Accepted: 2 May 2022

Published: 9 May 2022

**Publisher's Note:** MDPI stays neutral with regard to jurisdictional claims in published maps and institutional affiliations.



**Copyright:** © 2022 by the authors. Licensee MDPI, Basel, Switzerland. This article is an open access article distributed under the terms and conditions of the Creative Commons Attribution (CC BY) license (<https://creativecommons.org/licenses/by/4.0/>).

## 1. Introduction

The production and preservation of the juvenile continental crust are mainly associated with tectonic processes in complex zones of lithosphere-asthenosphere interplay

such as convergent plate margins [1]. The recognition of the involvement of crustal and mantle sources in the generation and evolution of the juvenile continental crust may be determined using whole-rock geochemistry data [2,3] and Sm-Nd isotopes [4] from arc magmatic rocks. Mantle input in magmatic arcs and back-arc basins largely results in material being transferred to the mantle through subduction [5]. However, because recycling in subduction zones provides a substantial contribution to establishing mantle compositional heterogeneities [6], it is expected that mantle-derived magmas may have different geochemical and isotopic signatures. Furthermore, the introduction of a juvenile component into arc-related granitic rocks could influence the contribution of a more greatly enriched old continental lower crust and the subcontinental lithospheric mantle (SCLM) [7,8] and even a more greatly depleted source derived from the deep asthenospheric mantle underlying the subducted oceanic lithosphere during the opening of the slab window [9].

In southwestern Iberia, a tectonic boundary separates Paleozoic terranes representing the Gondwana (Ossa-Morena Zone, OMZ) and Laurussia (Pulo do Lobo and South Portuguese zones) continental margins. These two continental margins progressively collided over the period from the Devonian to the Carboniferous during Pangea supercontinent assembly to form the Appalachian-Variscan belt [10–16] (Figure 1a). This complex tectonic boundary is produced by Late Carboniferous strike-slip faults separating the Pulo do Lobo Zone from Beja-Acebuches amphibolites and the Beja Igneous Complex (Figure 1b).

This has been interpreted as the suture zone of the Rheic Ocean that closed in the Late Devonian [13,17] and was then reworked during the Carboniferous, while the proposed subduction of the Paleotethys Ocean was taking place [16,18]. In a recently proposed model for the tectonic evolution of southwestern Iberia [16,18], after the closure of the Rheic Ocean in Devonian times, the subduction of the Paleotethys Ocean was initiated and proceeded during the Carboniferous. According to this tectonic model, in the first place, the OMZ is regarded as having acted as the lower plate during Rheic Ocean subduction, with the formation of a Devonian magmatic arc on the Laurussia margin (Pulo do Lobo and South Portuguese zones). Later, in the Carboniferous, the OMZ formed the upper plate during the subduction of the Paleotethys Ocean, creating ideal conditions for the emergence of a new magmatic arc.

The OMZ southwestern-most domain contains extensive exposures of Carboniferous arc-related igneous rocks, which have been studied over the last 15 years [16,18–29]. Despite some progress having been achieved, the timing and viability of the tectonic setting as related to the origin of such arc magmatic rocks are not yet fully understood. Indeed, little information has been compiled or examined on the chemical composition and age of key outcrops of a Late Carboniferous volcanic-subvolcanic suite from the Beja Igneous Complex (Baleizão porphyry and Alcáçovas dioritic rocks; [30–32]), occupying an area of about 500 km<sup>2</sup> in southwestern Iberia (Figure 1b). In this paper, a sampling survey was conducted on Carboniferous magmatic rocks of the Beja Igneous Complex with the aim of complementing previous geochemical and geochronological studies. We present new results for whole-rock geochemistry (analyses of major and trace elements) and Sm-Nd isotopic geochemistry for Baleizão porphyry and Alcáçovas dioritic rocks. Furthermore, we present the first SHRIMP U-Pb zircon geochronology data for Alcáçovas quartz diorite. The results obtained allowed us to (i) achieve a better estimate of the time scale of Carboniferous arc magmatism in the OMZ and (ii) improve on a recently suggested tectonic model and thus provide a better understanding of the sources of arc-related magmas within the framework of Paleotethys subduction during the Carboniferous.

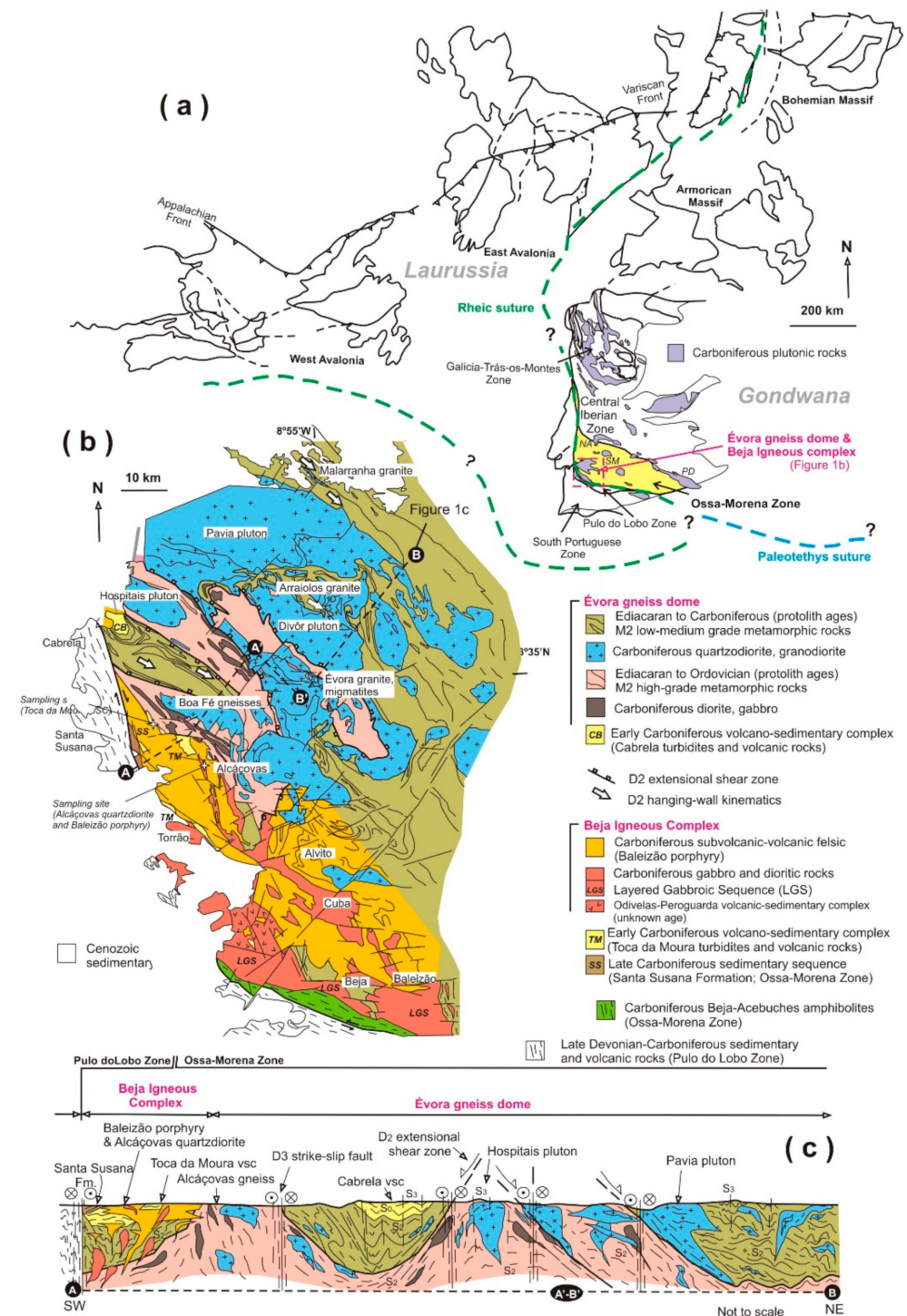


**Figure 1.** (a) Inset with the schematic location of Iberia in the Appalachian-Variscan belt in early Mesozoic times (adapted from [18]); location of the Beja Igneous Complex and the Évora gneiss dome (Ossa-Morena Zone, SW Iberia) in a schematic map showing the main Paleozoic tectonic units of Iberia. (b) Schematic geological map of the Beja Igneous Complex and the Évora gneiss dome (adapted from [33]). (c) Schematic cross-section through the Évora gneiss dome, Beja Igneous Complex and the tectonic boundary with the Pulo do Lobo Zone.

## 2. Geological Setting

The OMZ southwestern-most domain includes (i) the Evora Massif, representing a Carboniferous gneiss dome [34,35], and (ii) Carboniferous magmatic rocks of the Beja

Igneous Complex [22,23] (Figure 1). The oldest rocks of the Évora gneiss dome are the Ediacaran siliciclastic rocks of the Série Negra Group, derived from the denudation of a Cadomian magmatic arc [36,37]. The Ediacaran Série Negra Group is overlain by Cambrian-Ordovician siliciclastic and carbonate rocks associated with rift-related bimodal volcanic rocks [38,39]. This stratigraphy is recognized in other OMZ domains [40–42] where the metamorphic grade and associated extensional deformation intensity are not as great as in the Évora gneiss dome.

Crustal extension and doming ( $D_2$ ; Early Carboniferous) is superimposed on an initial event of crustal thickening ( $D_1$ ; Late Devonian) whose structures are only recognizable with difficulty [33].  $D_2$  extensional deformation was followed by another event of crustal thickening ( $D_3$ ; Late Carboniferous) that caused the upright folding of  $D_2$  foliation, thrusting and strike-slip faulting [34,43]. The Évora gneiss dome presents a large volume of Carboniferous granites and quartz diorites, and minor gabbro-diorites rocks with calc-alkaline signature [18,24–27,44]. These plutonic rocks are emplaced in metamorphic basement rocks, mainly composed of quartz-felspathic gneisses and migmatites, sheared under Buchan-type metamorphic conditions [33,34,43] (Figure 1b,c).

Visean turbiditic rocks and interbedded mafic and felsic volcanic rocks with calc-alkaline signature dated at ca. 335 Ma (Cabrela volcano-sedimentary complex [16]) represent the youngest stratigraphic unit found in the Évora gneiss dome (Figure 1b). Visean turbidites unconformably overlie the metamorphic basement rocks of the Évora gneiss dome [33]. Alcáçovas gneisses are representative of the metamorphic basement rocks that are intruded by magmatic rocks of the Beja Igneous Complex [45]. The Beja Igneous Complex is composed of (i) gabbro-dioritic rocks and granites dated at ca. 353–345 Ma from the Layered Gabbroic Sequence of the Odivelas-Beringel Complex and the Cuba-Alvito Complex; [21–23]), representing a magmatic event that is barely present in the Évora gneiss dome, and (ii) porphyries (Baleizão porphyry; Figure 2e–g) dated at ca. 318 Ma [16], minor granophyres, rhyolitic breccias and dioritic rocks (Figure 2h,i). The Beja Igneous Complex also includes mafic-intermediate volcanic rocks (the Odivelas-Peroguarda volcano-sedimentary complex), which have been tentatively assigned a Devonian age [39,46] although there are no radiometric ages confirming this interpretation. Baleizão porphyry intrudes and overlies a sequence of Visean turbidites alternating with mafic-intermediate (pillow-lavas; Figure 2a,b) and felsic volcanic rocks (Figure 2c,d) with calc-alkaline signature [46] dated at ca. 334–332 Ma (Toca da Moura volcano-sedimentary complex with a stratigraphic age correlative of the Cabrela volcano-sedimentary complex; [16]) (Figure 1b). Both Visean Toca da Moura sedimentary and volcanic rocks and Bashkirian Baleizão porphyry lie beneath a continental siliciclastic sequence composed of sandstone and shales with coal seams (Santa Susana Formation; [45,47,48]) that contain Kasimovian-Gzhelian conglomerates with pebbles of porphyry and Bashkirian-Moscovian (ca. 318–315 Ma) detrital zircon grains [16,49].

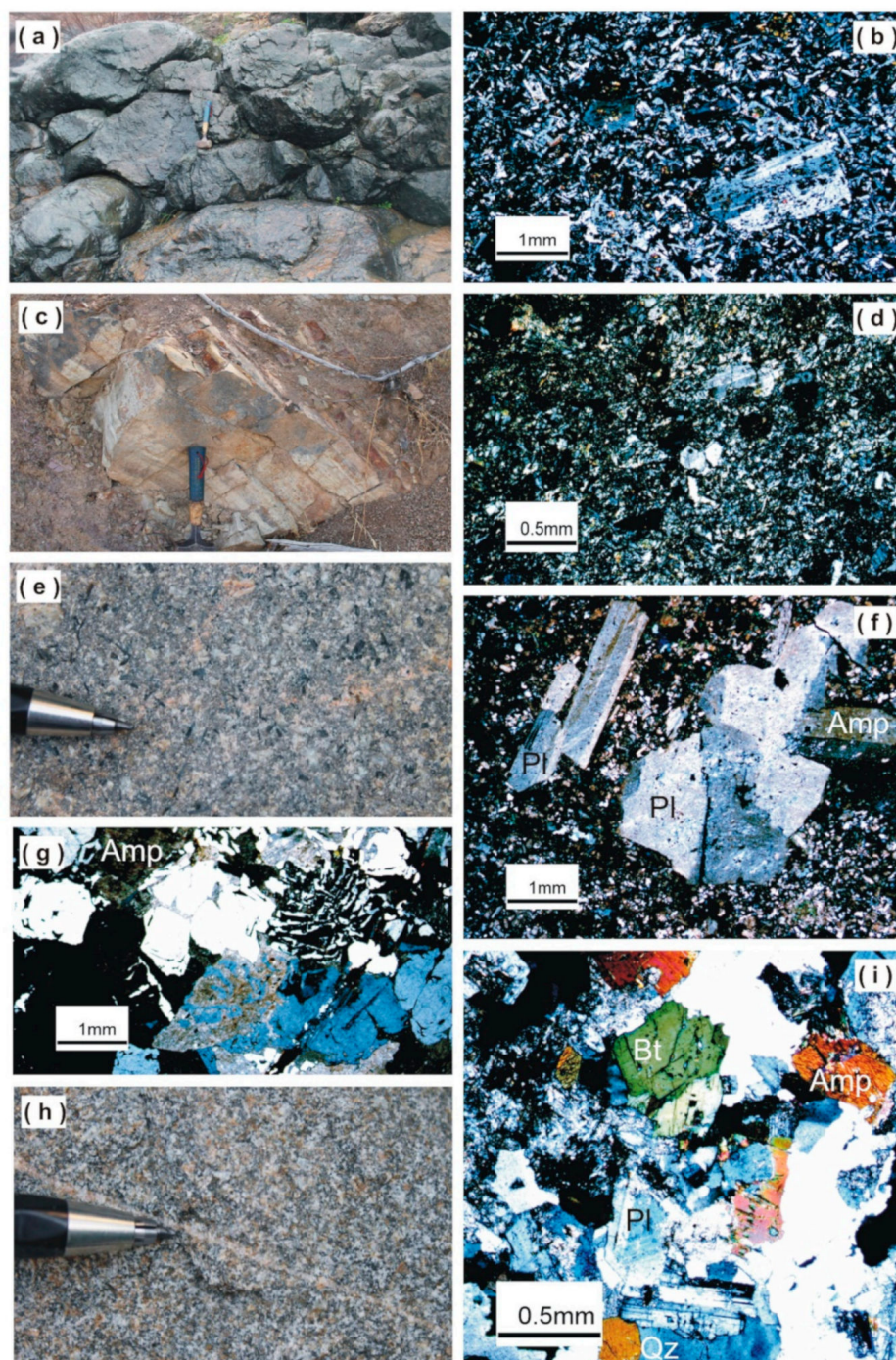


**Figure 2.** Toca da Moura volcano-sedimentary complex (Visean): (a) Mafic pillow-lavas; (b) microphotograph of a trachyandesite; (c) Felsic lavas; (d) microphotograph of rhyolite; (e) Baleizão porphyry (Bashkirian); (f,g) microphotographs showing plagioclase and amphibole phenocrysts surrounded by a fine-grained quartz-feldspathic matrix, and intergrowths of quartz and K-feldspar; (h) fine-grained Alcaçovas quartz diorite (Bashkirian); (i) microphotograph showing zoned plagioclase, amphibole, biotite and quartz.

### 3. Results

In this study, a set of nine fresh samples of igneous rocks from the Beja Igneous Complex (Visean Toca da Moura volcano-sedimentary complex and Bashkirian Baleizão porphyries and Alcaçovas quartz dioritic rock) was analyzed for major and trace elements and Sm-Nd isotopes. Furthermore, SHRIMP U-Pb analyses were performed for the first

time on magmatic zircon from Alcáçovas quartz diorite to validate the age relation with spatially associated Baleizão porphyries. Toca da Moura volcanic rocks and Baleizão porphyries were sampled from selected exposures from the River São Cristovão, the River Alcáçovas and the Pêgo do Altar Reservoir. Alcáçovas quartz diorite was sampled from a site located 2 km west of the village of Alcáçovas. Analytical results are listed in Tables S1–S3 (Supplementary Materials) and shown in Figures 3–7. Analytical methods are described in Section S4 (Supplementary Materials).

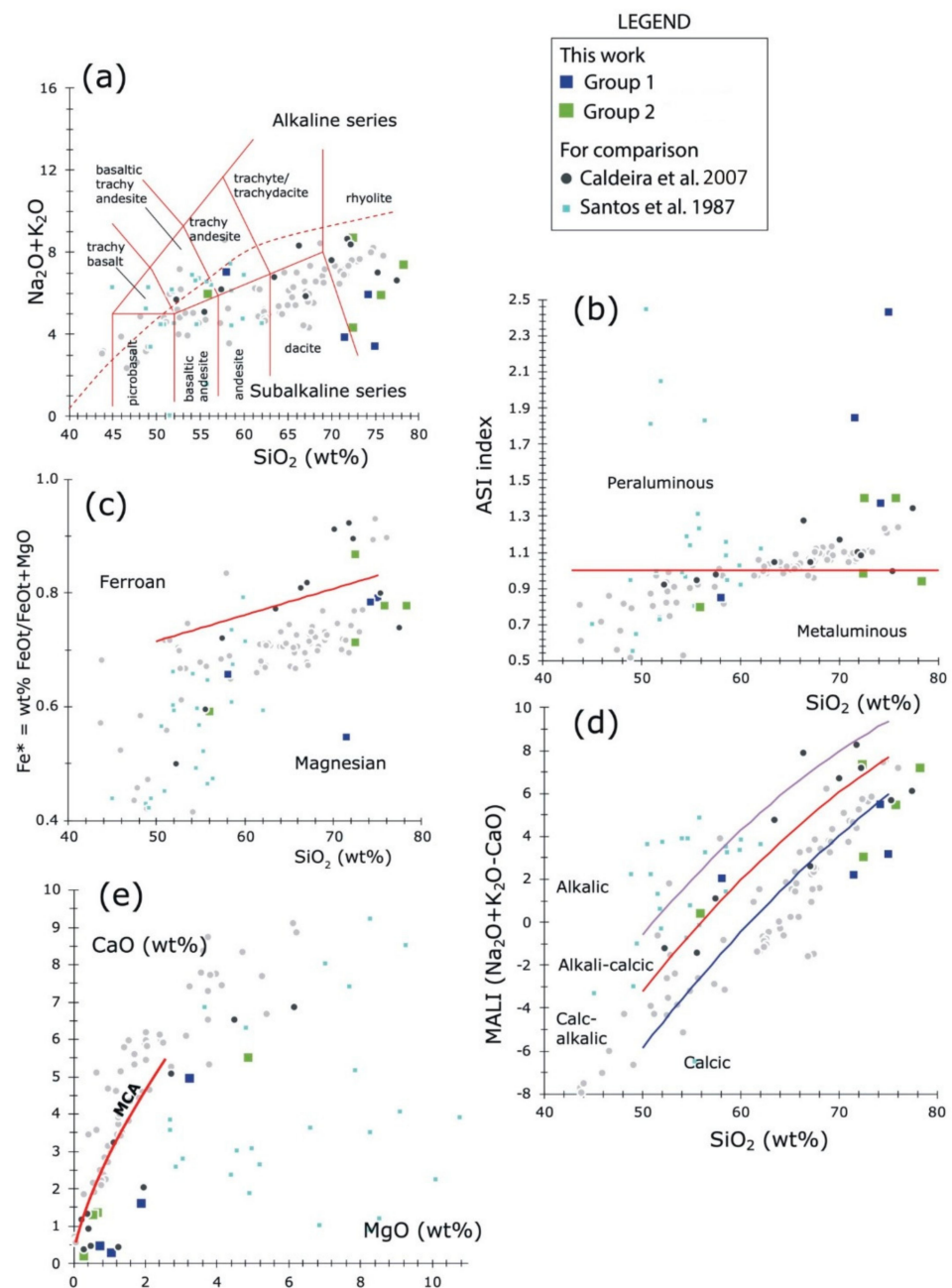


**Figure 3.** Main geochemical classification diagrams for the Toca da Moura (Group 1) and Baleizão-Alcáçovas (Group 2) igneous rocks. Grey dots represent the Évora gneiss dome plutonic rocks [18,24,25,27]. (a) TAS diagram shows the subalkaline character of these rocks. Alumina saturation index (ASI); (b) and the Fe number (c) becomes greater as the silica content increases. (d) Modified alkali-lime index (MALI) vs  $\text{SiO}_2$  diagram indicates the alkali-calcic and calcic trends of the samples. (e) CaO vs. MgO diagram shows the departing of the Toca da Moura and Baleizão-Alcáçovas igneous rocks from the Main Cotectic Array (MCA).

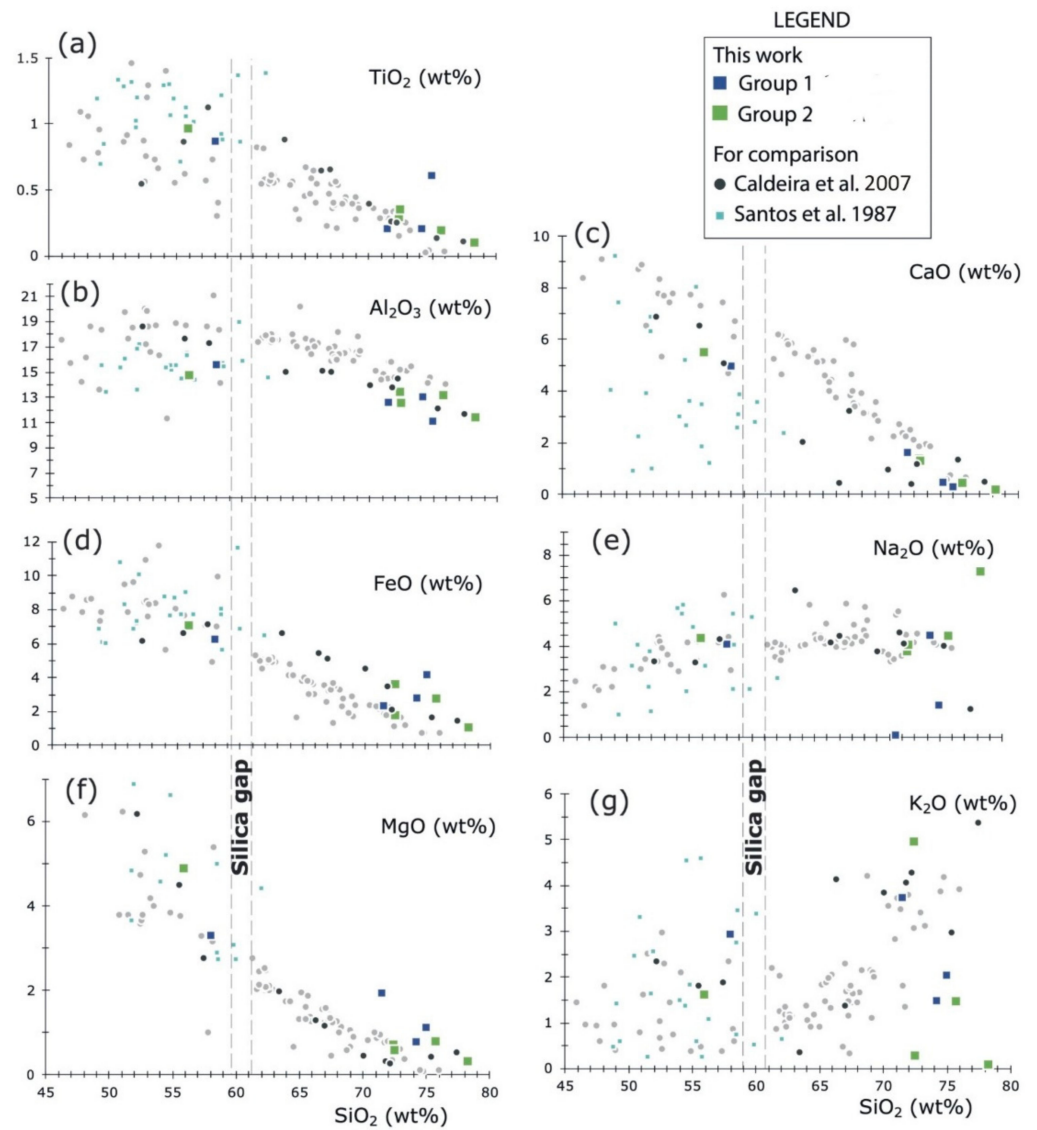


**Figure 4.** Harker diagrams for the Toca da Moura (Group 1) and Baleizão-Alcáçovas (Group 2) igneous rocks showing the main geochemical variations on (a) TiO<sub>2</sub>, (b) Al<sub>2</sub>O<sub>3</sub>, (c) CaO, (d) FeO, (e) Na<sub>2</sub>O, (f) MgO and (g) K<sub>2</sub>O contents. Grey dots are as in Figure 3.

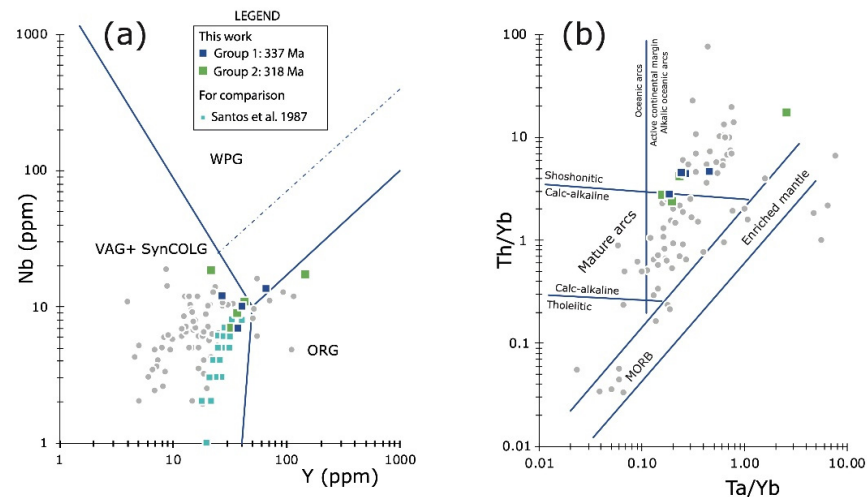


**Figure 5.** Cont.

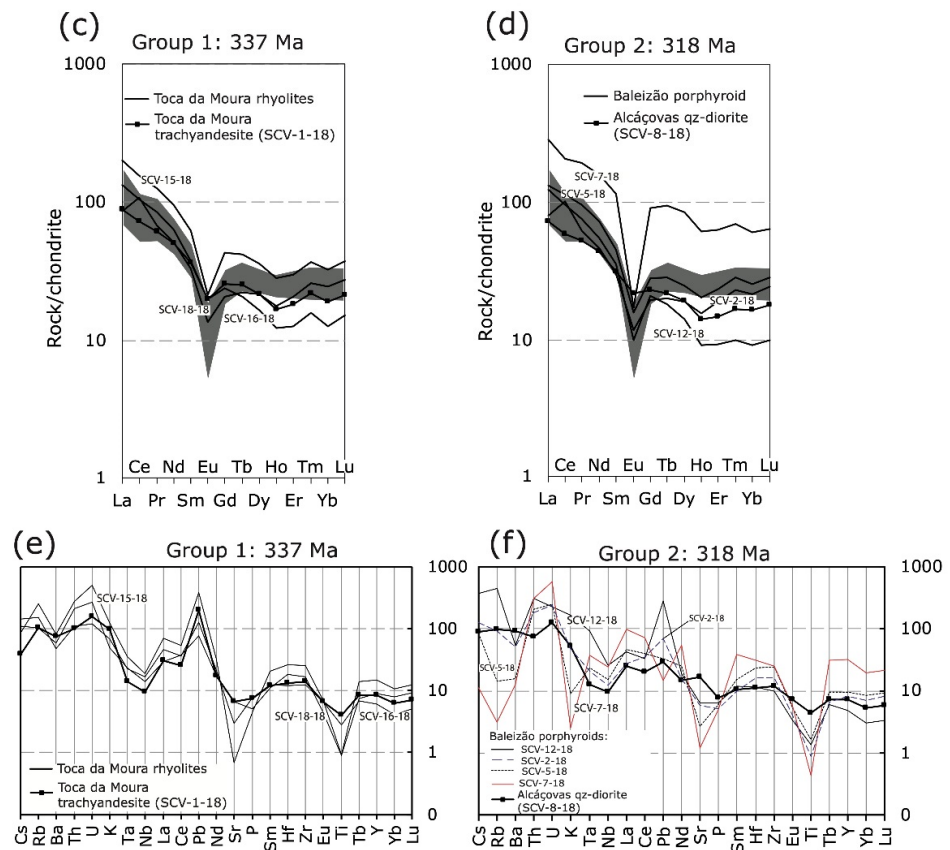


**Figure 5.** (a) Y vs. Nb diagram [52] discriminating between volcanic arc granite and syncollisional granites (VAG+SynCOLG), within plate granites (WPG) and orogenic granites (ORG). Data of the Baleizão porphyries ([20]; grey dots) and the Toca da Moura mafic-intermediate volcanic rocks ([50]; light blue squares) are used for comparison. (b) Ta/Yb vs. Th/Yb diagram [51] shows the geochemical affinity with active continental margin magmatism. Data of Baleizão porphyries from Alvito, Torrão and Alcáçovas regions [20] are used for comparison (grey dots). (c,d) Chondrite normalized rare earth element (REE) diagrams showing the main REE patterns of the Toca da Moura (Group 1) and the Baleizão-Alcáçovas (Group 2) igneous rocks. Data of Baleizão porphyries from Alvito, Torrão and Alcáçovas regions [20] are used for comparison (grey zone). (e,f) Primitive mantle-normalized trace elemental patterns of Group 1 and 2 igneous rocks.

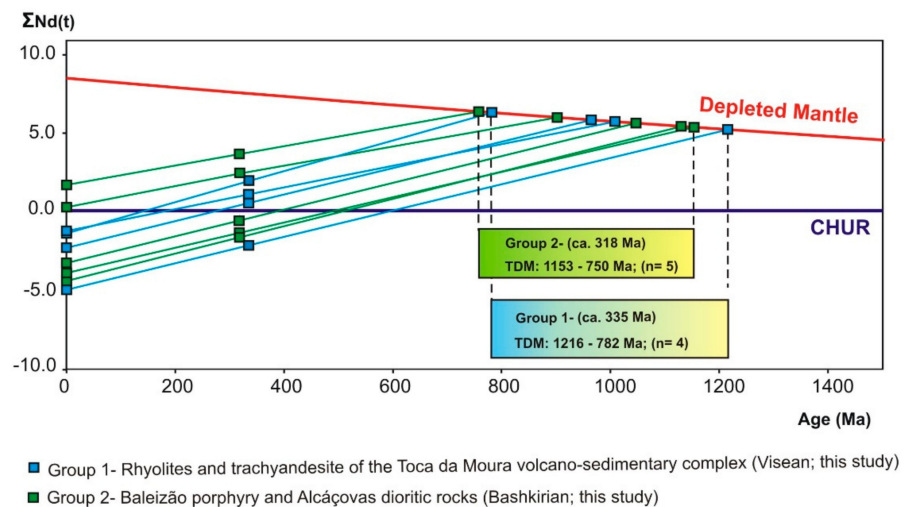


**Figure 6.** Nd  $T_{DM}$  model ages [53] for the Toca da Moura (Group 1) and Baleizão-Alcáçovas (Group 2) igneous rocks.



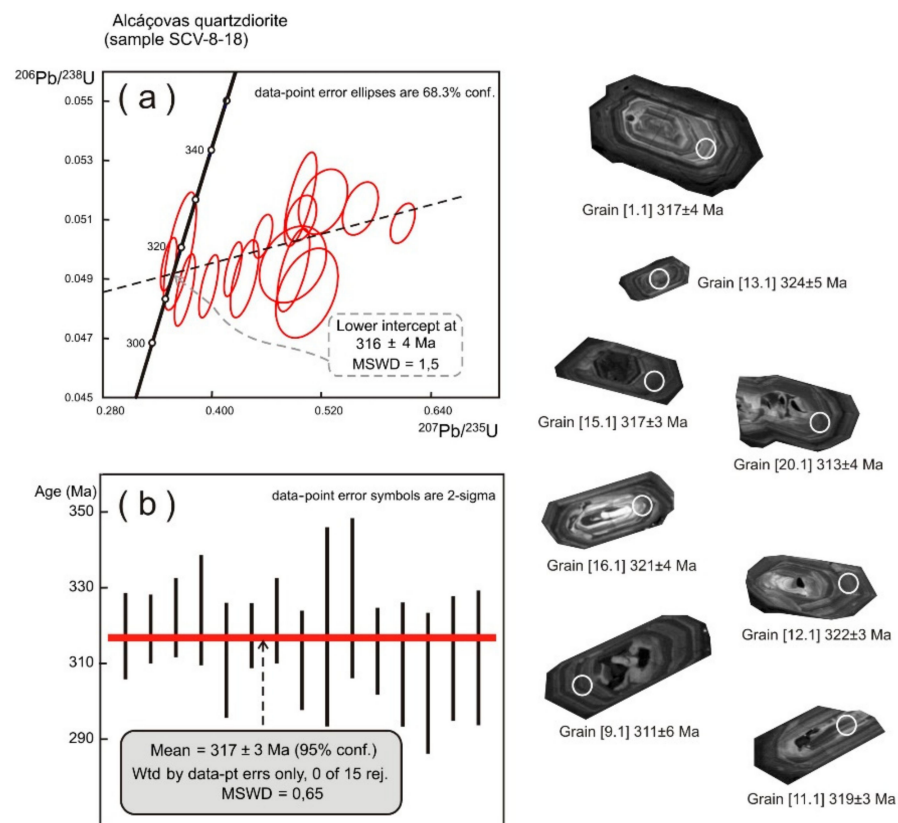


**Figure 7.** Concordia diagram and weighted mean of  $^{206}\text{Pb}/^{238}\text{U}$  ages of analyzed zircon grains of the Alcáçovas quartz diorite. Cathodoluminescence images of representative zircon grains. Circle-analytical spot of approximately 25 micra. (a) Concordia plot; (b) weighted mean of 15  $^{206}\text{Pb}/^{238}\text{U}$  ages.

### 3.1. Whole-Rock Geochemistry and Petrography

Major and trace element compositions of Group 1 (ca. 335 Ma [16]) including Toca da Moura volcano-sedimentary complex mafic (1 sample: SCV-1-18) and felsic (3 samples: SCV-12-18, SCV-16-18 and SCV-18-18) rocks, and Group 2 (ca. 318 Ma, [16]) comprising Baleizão porphyry (4 samples: SCV-2-18, SCV-5-18, SCV-12-18 and SCV-7-18) and Alcáçovas dioritic rock (1 sample: SCV-8-18) are shown in Table S1 (Supplementary Materials). The new results obtained are plotted in Figures 3–5 together with data previously published by other authors, for the purpose of comparison.

Samples from the Beja Igneous Complex plot into the sub-alkaline field (Figure 3a) and range from metaluminous to peraluminous according to the increase in silica (Figure 3b). Samples from Group 1 are classified as rhyolites (SCV-15-18, SCV-16-18 and SCV-18-18; silica content ranges from 72 to 75 wt%) and a trachyandesite (SCV-1-18; 58 wt%). Group 2 samples are mainly classified as rhyolites (SCV-2-18, SCV-5-18, SCV-7-18 and SCV-12-18, with  $\text{SiO}_2$  content from 72 to 78 wt%), close to dacitic composition.

Almost all samples are classified as magnesian (Figure 3c), and they vary from alkali-calcic to calcic according to the MALI index (Figure 3d). Igneous rocks from the Beja Igneous Complex do not follow the main cotectic array (MCA in Figure 3e) or the Évora magmatism trend. Harker diagrams display a good correlation for higher silica content and scattered values for the low-silica end of the series, except for  $\text{Na}_2\text{O}$  and  $\text{K}_2\text{O}$ , neither of which show any correlation with  $\text{SiO}_2$ . Both groups, igneous rocks from ca. 335 Ma and ca. 318 Ma [16], have silica-poor members (andesitic,  $\text{SiO}_2 < 60$  wt%) associated with higher  $\text{MgO}$ ,  $\text{FeO}$ ,  $\text{TiO}_2$  and  $\text{CaO}$  content than silica-rich compositions ( $\text{SiO}_2 > 70$  wt%), having high alkali content (Figure 4). The variability of the major element ( $\text{Mg}$ ,  $\text{Ca}$ ,  $\text{K}$  and  $\text{Na}$ ) content of Toca da Moura mafic-intermediate volcanic rocks is probably associated with the metasomatic exchange

between igneous precursors and hydrothermal fluids. Metasomatism was produced, resulting in the albitization, sericitization and carbonatization of pillow-lavas [50].

REE patterns are marked by Eu negative anomalies (Figure 5). Trachyandesite and quartz diorite present similar patterns, which are less pronounced than those of rhyolites and porphyroids (Figure 5c,d). Almost all samples are classified as volcanic arc and syn-collisional granites (Figure 5a) and plot into the field of active continental margin (Figure 5b) in accordance with [51,52]. Groups 1 and 2 show similar abundances of fluid immobile elements such as Nb-Ta and Zr-Hf (Figure 5f,g).

Porphyries contain phenocrysts of quartz, albite, K-feldspar, amphibole, and biotite, sometimes reaching 3 mm in diameter and forming mineral aggregates, surrounded by a very fine-grained quartz-feldspathic matrix with opaque minerals. In coarse-grained samples, quartz and feldspar angular intergrowths, such as those typical of granophyric texture, are recognized (granophyre). Feldspar phenocrysts almost always show hydrothermal alteration, with the growth of sericite and opaque minerals, whereas amphibole and biotite phenocrysts are partially replaced by chlorite and epidote. Sample SCV-8-18 ( $\text{SiO}_2 = 56 \text{ wt}\%$ ), which falls into the basaltic trachyandesite field, shows a phaneritic texture, and plagioclase, amphibole, quartz and biotite are identified; it is classified as a quartz dioritic rock.

### 3.2. Sm-Nd Isotope Chemistry Data

The Sm-Nd isotope compositions of magmatic rocks from Group 1 (ca. 335 Ma; 4 samples) and Group 2 (ca. 318 Ma; 5 samples) are shown in Table S2 (Supplementary Materials). Initial  $^{143}\text{Nd}/^{144}\text{Nd}$  ratios, ranging from 0.512094 to 0.512416, show differences between the two groups of calc-alkaline rocks. Samples SCV-1-18 (trachyandesite), SCV-15-18 and SCV-16-18 (rhyolites) belonging to the Toca da Moura volcano-sedimentary complex (Group 1) display positive  $\epsilon\text{Nd}(t)$  values ranging from +0.5 to +1.9, corresponding to depleted mantle model ( $T_{\text{DM}}$ ) ages of 782–1009 Ma (Table S2). The only exception is sample SCV-18-18 (rhyolite), with negative  $\epsilon\text{Nd}(t) = -2.2$ , corresponding to the older  $T_{\text{DM}}$  age of 1216 Ma. Samples from Group 2 also display positive and negative  $\epsilon\text{Nd}(t)$  values (Table S2 and Figure 6) but show different values than Group 1. Samples SCV-7-18 (Baleizão porphyry) and SCV-8-18 (Alcáçovas Qz-dioritic rock) of Group 2 show the higher  $\epsilon\text{Nd}(t)$  values of +2.4 and +3.2, related to  $T_{\text{DM}}$  ages of 902 and 758 Ma, respectively. The other samples of rhyolitic composition of the Baleizão porphyry (Group 2) present negative  $\epsilon\text{Nd}(t)$  values ranging from  $-1.5$  to  $-0.6$  and  $T_{\text{DM}}$  ages from 1047 to 1153 Ma. The higher  $T_{\text{DM}}$  ages of samples SCV-18-18 (Group 1), SCV-2-18, SCV-5-18 and SCV-12-18 (Group 2) suggest a higher degree of continental crustal contamination.

### 3.3. U-Pb Zircon Geochronology Data

Alcáçovas fine-grained dioritic rock (sample SCV-8-18) consists of hornblende, plagioclase, biotite, quartz and K-feldspar. It is characterized by a zircon population containing subhedral to prismatic euhedral grains (50–160  $\mu\text{m}$  in diameter). Prisms are equant to moderately elongated, showing a simple internal structure characterized by concentric zoning or revealing a variable-width concentric zoned rim surrounding unzoned, banded or complex zoning cores (composite grains). A total of 22 U-Th-Pb SHRIMP analyses for sample SCV-8-18 yielded a U content ranging from 427 to 5713 ppm (Table S3, Supplementary Materials). The 15 grains in the  $^{208}\text{Pb}/^{238}\text{U}$  age range ca. 327–305 Ma ( $^{208}\text{Pb}$ -corrected and with discordance  $< 10$ ) yielded a weighted mean age of  $317 \pm 3 \text{ Ma}$  (MSWD = 0.65; Figure 7b), which is the best estimate for the crystallization age of Alcáçovas quartz diorite. This estimation is slightly older than the age of  $316 \pm 4 \text{ Ma}$  (MSWD = 1.5; Figure 7a) obtained from the lower intercept of the Concordia curve for common lead uncorrected  $^{208}\text{Pb}/^{238}\text{U}$  ages (discordance  $< 30$ ) and overlaps with the age of  $318 \pm 2 \text{ Ma}$  recently obtained for Baleizão porphyry [16].

#### 4. Discussion: Sources of the Carboniferous Magmatic Arc

The compositional variability of OMZ Carboniferous calc-alkaline magmatic rocks may reflect the contribution of various types of magma sources. There is an almost complete absence of silica of around 60 wt% (Figure 4 and Table S1), which is common for the igneous rocks from Évora magmatism. Group 1 trachyandesite (sample SCV-1-18) and the same age mafic and intermediate-mafic rocks of the Toca da Moura volcano-sedimentary complex [50], Group 2 quartz diorite (sample SCV-8-18) and the dioritic rocks of Alvito-Alcáçovas [20] represent samples with a SiO<sub>2</sub> content lower than 60 wt%. These rocks may represent residues in the fractionation process, whereas compositions with SiO<sub>2</sub> > 60 wt% correspond to differentiated liquids from Évora magmatism.

The REE-pattern is similar to that associated with previous data for Baleizão porphyries [20] (Figure 5c,d). The prominent negative Eu anomaly is indicative of plagioclase present in a residue or cumulate. Figure 5a,b show that Toca da Moura rhyolites and Baleizão porphyries (including data from [20]) have a low Nb and Ta content relative to neighboring elements, typical of subduction-related magmas [52]. For the purpose of comparison, Baleizão porphyries, Alvito-Alcáçovas dioritic rocks [20] and Toca da Moura intermediate-mafic volcanic rocks [50] are also plotted in the VAG+SynCOLG field in accordance with the Nb vs. Y tectonic discriminating diagram [52] (Figure 5a), increasing the likelihood that these rocks may have been generated in magmatic arcs. Furthermore, in the Th/Yb vs. Ta/Yb diagram for basalts generated in distinct tectonic settings [51], samples of Groups 1 and 2 share the same continental arc magmatic signature as most of the plutonic rocks of the Évora gneiss dome (Figure 5b). The compositional link between Groups 1 and 2 is also demonstrated by their Primitive mantle-normalized trace elemental patterns (Figure 5e,f).

Our geochemical, isotopic and geochronological findings allowed us to (i) complement previous information about Visean and Bashkirian magmatism in the OMZ; (ii) establish the timing and the compositional changes of Carboniferous arc-related magmatism in the OMZ; and (iii) discuss the tectonic framework of OMZ Carboniferous magmatism during the process of the convergence of the Laurussian and Gondwanan continental margins; this Carboniferous arc magmatism was probably emplaced in the OMZ (upper plate) immediately after the closure of the Rheic Ocean, following the onset and development of the Paleotethys subduction. From the perspective of the temporal and spatial transition from one locally superimposed orogenic cycle to another, it may be assumed that the onset of Carboniferous OMZ arc magmatism may have overlapped chronologically with (i) the magmatic activity recognized in the South Portuguese Zone (i.e., Pyrite belt) that took place after the Laurussia-Gondwana collision (i.e., Variscan orogeny) as a result of the slab break-off of the Rheic oceanic lithosphere beneath the Laurussian margin during the Tournaisian [23]; and (ii) the production of magmatism in the Central Iberian and West Asturian-Leonese zones that mainly derived from the extensional collapse of the Variscan orogen in the Serpukhovian-Bashkirian [53–55], and the subsequent development of the Iberian orocline from Moscovian to Gzhelian times [56,57].

In this discussion, we assume that the geochemical and isotopic pattern of OMZ Carboniferous magmatic rocks may result from the Paleotethys subduction process (i.e., ocean-continent convergence), as observed in modern analogues of the Pacific region, and consequently, that it is not directly associated with Variscan collision (i.e., continent-continent convergence).

Calc-alkaline magmas could have derived from melting of mélangé diapirs that carried fertile subducted materials into hot regions of the supra-subduction mantle wedge under the SCLM during the Paleotethys subduction; likewise, this is described for Cordilleran-type Batholiths [58]. Similar composition melts could also have resulted from the product of crustal recycling of the magmatic arc roots formed during the initial stages of Paleotethys subduction [18]. Furthermore, the origin of calc-alkaline magmas linked to the inherited compositional signature of an older Cadomian (Ediacaran) subduction process transferred to the SCLM beneath the OMZ, which then became the source, or a source component, has been recognized for other regions of Iberia [59]. Enriched magma sources derived from

successive subduction processes are not easy to distinguish from each other. However, because some Carboniferous OMZ mafic rocks show negative  $\epsilon\text{Nd}(t)$  values and older depleted mantle model ages than Ediacaran-Ordovician OMZ mantle-derived igneous rocks (a proxy for the isotopic composition of the SCLM beneath the OMZ; see discussion below), it may be assumed that Paleotethys subduction played a role in the contamination of the sub-continental mantle. In contrast, the presence of mafic rocks (Acebuches MORB amphibolites; [60]) with very high  $\epsilon\text{Nd}(t)$  values compared to those of the SCLM under the OMZ suggests the involvement of a putative highly depleted mantle source. This high depleted magma probably derived from the asthenospheric mantle beneath the subducted Paleotethys ridge. Thus, the different components that may have contributed with depleted or enriched magmas derived from the mantle do not seem to have been the only cause of the compositional variability of Carboniferous arc-related magmatic rocks. The contribution of enriched magma sources is most likely derived from the partial melting of older (Ediacaran-Cambrian) metasedimentary and metaigneous country rocks with a calc-alkaline signature [24], also indicative of crustal contamination in the Carboniferous.

#### 4.1. Tournaisian: Earliest Stage of Arc-Magmatism

The oldest Carboniferous magmatism found in the OMZ is represented by the gabbro-dioritic rocks of the Tournaisian Layered Gabbroic Sequence [22,23] (Figure 1b). The geochemical and Sm-Nd isotopic features of Layered Gabbroic Sequence rocks suggest quite a complex process of petrogenetic evolution involving mixing processes between a time-integrated depleted mantle component (mafic cumulates show the most primitive isotope signatures) and some crustal end members (more evolved mafic rocks) [23]. Less LREE-enriched Tournaisian Beja and Torrão gabbro-dioritic rocks show positive  $\epsilon\text{Nd}(t)$  values of between +0.3 and +4.0 [22,23] and young Nd model ages ranging from 1057 to 754 Ma, suggesting derivation from a juvenile mantle source (Figure 8). The Nd isotopic composition of Tournaisian Beja and Torrão gabbro-dioritic rocks is remarkably similar to that of Ediacaran-Ordovician OMZ mantle-derived intermediate (ca. 540 Ma, Ediacaran Cordoba andesites,  $\epsilon\text{Nd}(t) = +2.9$  to  $+6.1$  and  $T_{\text{DM}}$  ages = 624–958 Ma, [61]), mafic (ca. 510 Ma, Middle Cambrian Main Rift Event basalts,  $\epsilon\text{Nd}(t) = +2.4$  to  $+5.6$  and  $T_{\text{DM}}$  ages = 737–1037 Ma, [40]), and felsic and mafic (ca. 480 Ma, Early Ordovician Alter to Chão-Elvas gabbros and syenites,  $\epsilon\text{Nd}(t) = +2.5$  to  $+4.7$  and  $T_{\text{DM}}$  ages = 579–1048 Ma, [62]) magmatic rocks (Figure 8a). Cordoba andesites represent Cadomian arc-back-arc juvenile magmatism, whereas Mid-Cambrian OIB and MORB basalts and Ordovician alkaline-peralkaline mafic and felsic rocks characterize rift-related juvenile magmatism in the OMZ [40,41]. The Nd isotopic signature of Ediacaran-Ordovician OMZ mantle-derived igneous rocks may be regarded as a proxy of the isotopic composition of the SCLM beneath the OMZ, which did not change significantly from the Ediacaran to the Carboniferous. Besides this, the Nd isotopic signature of OMZ Cambrian-to-Carboniferous mafic rocks is indistinguishable from the evolutionary range defined for the SCLM isotopic composition of the Central Iberian, West Asturian-Leonese and Cantabrian zones. The involvement of enriched lithospheric mantle sources during the Cadomian and Variscan magmatism indicates the existence of an older (Proterozoic?) SCLM beneath central Iberia [63]. The SCLM beneath these tectonic zones of Iberia is characterized by positive  $\epsilon\text{Nd}(t)$  values and isotopic model ages ranging from 1100 Ma to 800 Ma [59]. However, negative  $\epsilon\text{Nd}(t)$  values and significantly older isotopic model ages found in the youngest Carboniferous mafic rocks suggest derivation from an SCLM contaminated by Late Paleozoic subduction [8]. This evolution of the mantle source beneath Gondwana is shared by most Variscan massifs [8], revealing some temporal and spatial isotopic variations along the orogen [63,64].

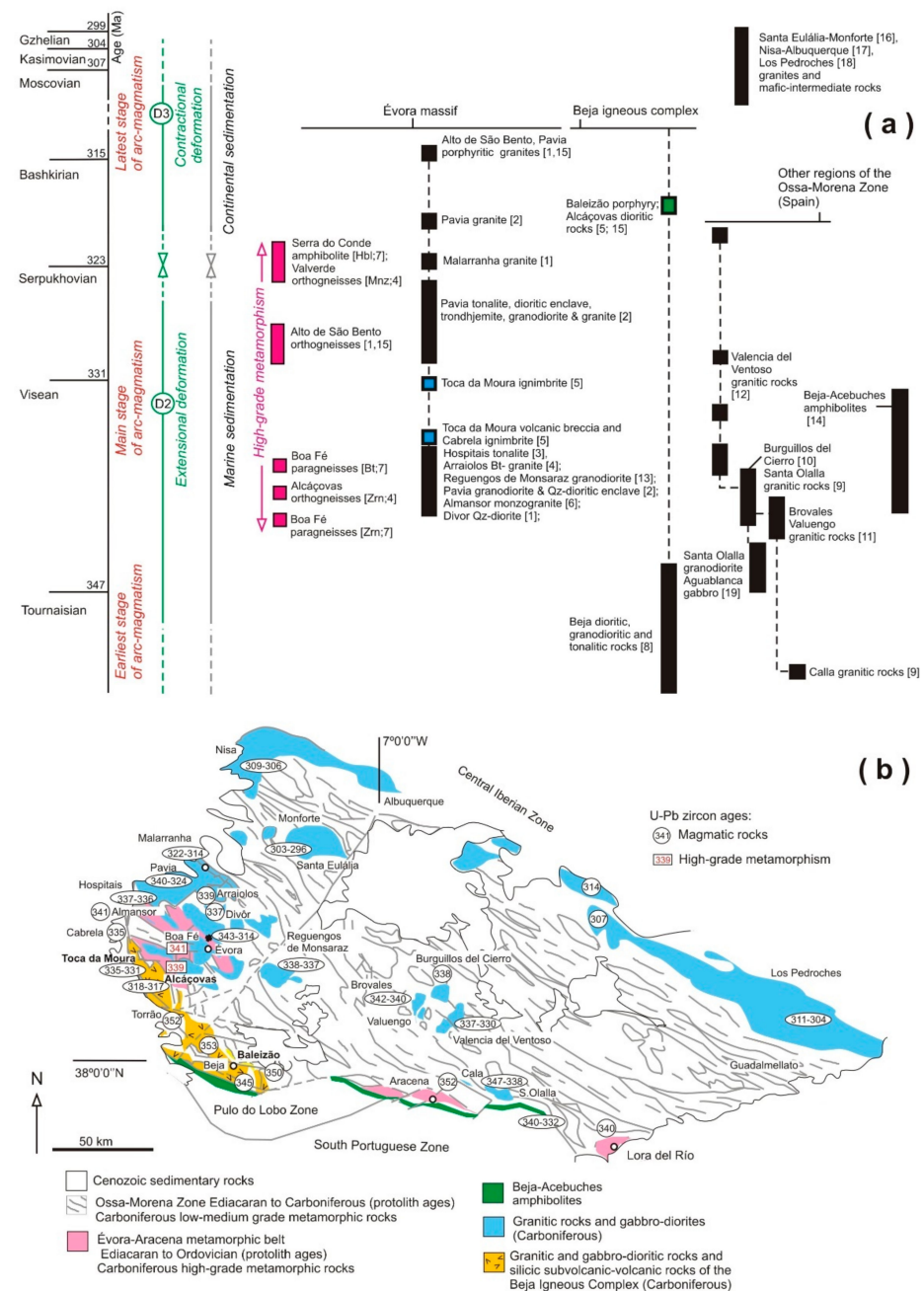


**Figure 8.** (a) Timeline of the stages of Carboniferous arc magmatism, and high-grade metamorphism, deformation, and sedimentation events, represented in the Ossa-Morena Zone (mostly focused on the Évora gneiss dome and the Beja Igneous Complex; geochronology data from: 1 [34]; 2 [26]; 3 [25]; 4 [33]; 5 [16]; 6 [44]; 7 [43]; 8 [23]; 9 [19]; 10 [67]; 11 [68]; 12 [29]; 13 [69]; 14 [70]; 15 [18]; 16 [71]; 17 [72]; 18 [73] and 19 [74]; compiled magmatic (black bars) and metamorphic (magenta bars) ages; U-Pg ages from this study (dark blue and green bars); (b) simplified geological map of the Ossa-Morena Zone showing a compilation of magmatism and metamorphism ages (adapted from [18,43]).

The evolution of the juvenile basaltic magmas from which the ca. 350 Ma Beja and Torráo mafic plutonic rocks (Figure 9) derived was probably associated with a degree of crustal contamination during ascent [22] and may have been dominated by fractional crystallization of mafic phases and plagioclase, combined with variable degrees of assimilation of silicate melts and hydrous fluids due to subduction of the oceanic lithosphere [23]. The origin and emplacement of the Layered Gabbroic Sequence have been ascribed to a process of slab break-off that followed the Devonian subduction of the Rheic oceanic lithosphere

and the collision of Laurussia and Gondwana [22,23]. As an alternative, we propose a distinct tectonic model for the emplacement of the Layered Gabbroic Sequence involving the first stage of a continental magmatic arc in the OMZ due to Paleotethys subduction (Figure 10a). Thus, immediately after the closing of the Devonian Rheic Ocean, the subduction of the Paleotethys oceanic lithosphere under the OMZ (upper plate) became active in Tournaisian times, resulting in the earliest stage of the emplacement of the arc-derived magmas of the Layered Gabbroic Sequence [16,18] (Figure 10b). As a consequence, the overriding of a mantle anomaly or enhanced decompression melting of the subcontinental lithospheric mantle could have favored extension and magma emplacement in the OMZ upper crust, causing volcanism in Tournaisian marine basins [65,66].

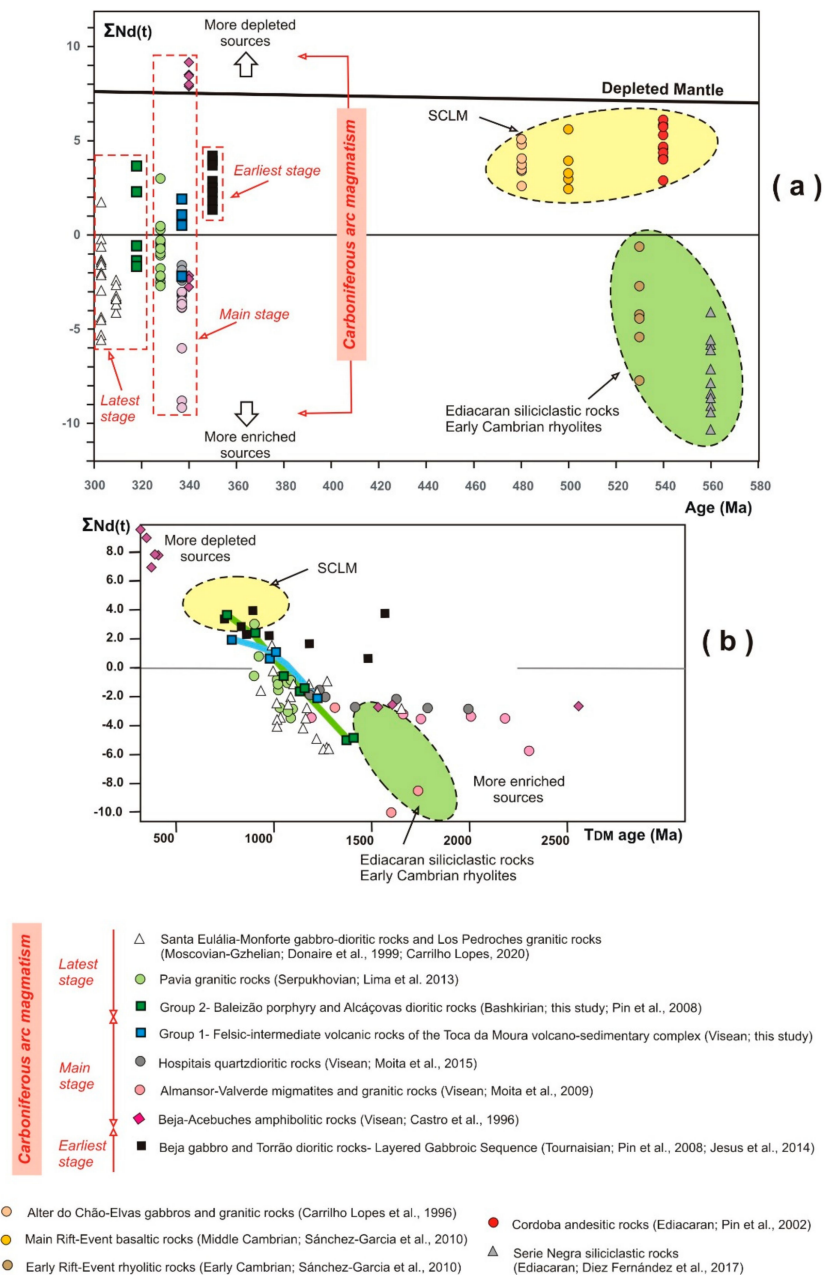


**Figure 9.** Compilation of bulk rock epsilon Nd values from Ossa-Morena Zone igneous and sedimentary rocks. SCLM-proxy for the isotopic composition of the SCLM beneath the Ossa-Morena Zone (see discussion in the text). (a)  $\epsilon Nd$  vs. age and (b)  $\epsilon Nd$  vs.  $T_{DM}$  age diagrams for the Toca da Moura (Group 1) and Baleizão-Alcáçovas (Group 2) igneous rocks and other relevant data from the Ossa-Morena Zone.

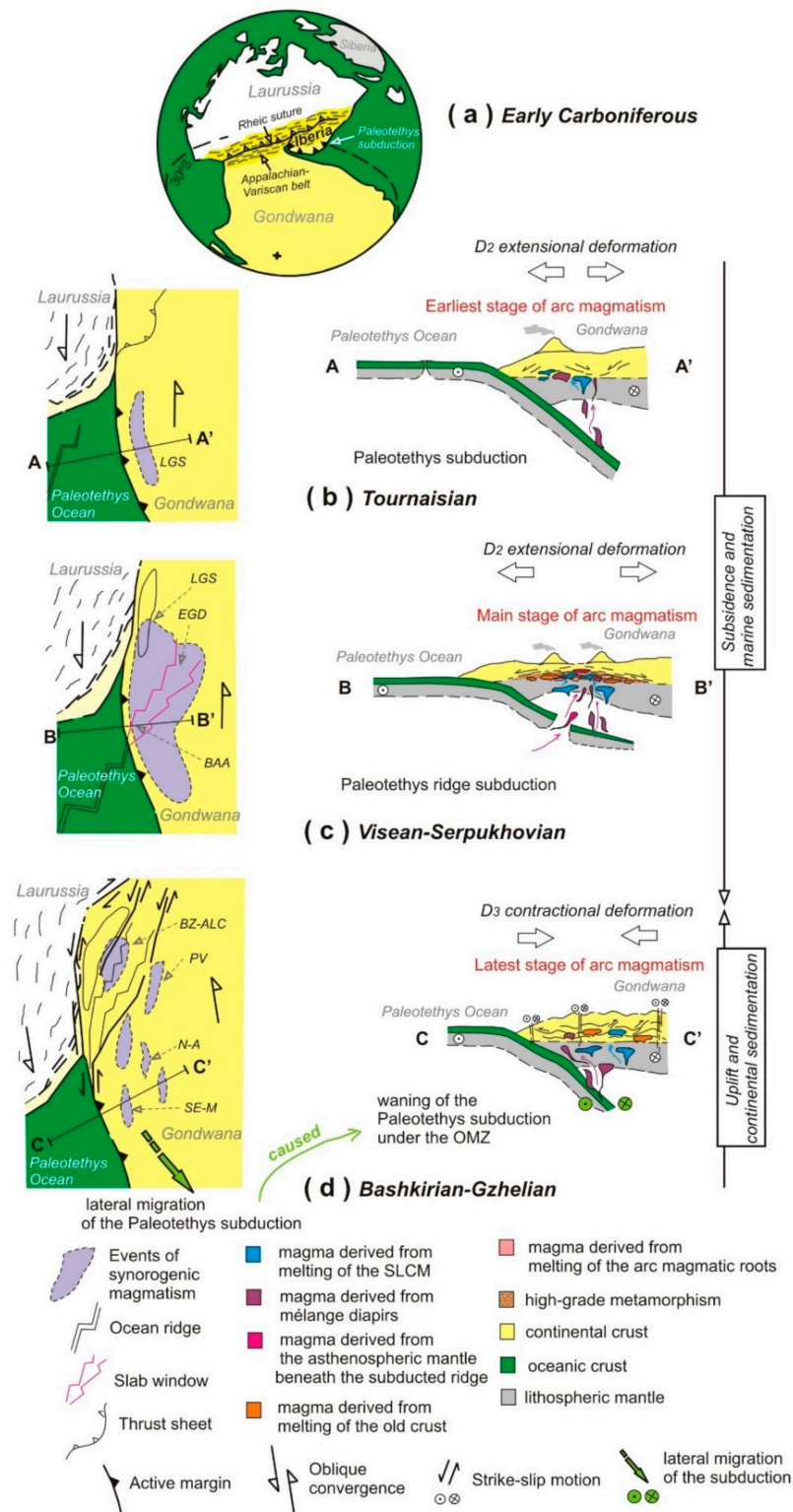


**Figure 10.** (a) Paleogeographic reconstruction for the Carboniferous showing the Appalachian-Variscan belt, the Rhenic suture and the Paleotethys subduction; (b–d) sketches showing assumed tectonic evolution recorded in SW Iberia, with the sequence of Carboniferous stages of arc magmatism that took place during the Laurussia-Gondwana oblique collision and the Paleotethys subduction (modified from [16,18]). BAA: Beja-Acebuches Amphibolites; BZ-ALC: Baleizão porphyries and Alcáçovas quartz diorites; Other Carboniferous OMZ plutonic rocks: EGD: Évora Gneiss Dome; LGS: Layered Gabbroic Sequence; N-A: Nisa-Albuquerque; PV: Pavia; PD: Los Pedroches; SE-M: Santa Eulália-Monforado.

#### 4.2. Visean-Serpukhovian: Main Stage of Arc-Magmatism

According to our tectonic model, the oblique convergence of Laurussia and Gondwana persisted during the Visean-Serpukhovian with Paleotethys ridge subduction under the OMZ [16]. As a result, the development of a slab window beneath the Gondwanan margin favored asthenosphere upwelling [18,60]. The newly established profound thermal anomaly this produced could have triggered the partial melting of crustal materials and lithosphere D<sub>2</sub> extension (Figure 10c), creating the right conditions for the development of gneiss domes in the OMZ [33,34,43]. The emplacement of voluminous calc-alkaline magmas from which the ca. 339–335 Ma granitic and gabbro-dioritic rocks of the Évora gneiss dome [18,24,25,34,44] derived is coeval with the intrusion of mafic-ultramafic rocks with a transitional composition between mid-ocean ridge basalts and island arc basalts [60,75] of ca. 340–332 Ma [68] Beja-Acebuches amphibolites (Figure 9). Most Almansor and Valverde granitic rocks and migmatites present negative  $\epsilon\text{Nd}(t)$  values ranging from  $-1.6$  to  $-9.2$  [24] and Nd model ages of 1191 to 2299 Ma, with some samples overlapping the range defined by Ediacaran Série Negra metasedimentary rocks ( $\epsilon\text{Nd}(t) = -4.1$  to  $-10.3$  and  $T_{\text{DM}}$  ages = 1491–1854 Ma [36]) and Cambrian Early Rift Event rhyolitic rocks ( $\epsilon\text{Nd}(t) = -2.9$  to  $-13.2$  and  $T_{\text{DM}}$  ages = 1426–1789 Ma [37]) (Figure 8). These negative  $\epsilon\text{Nd}(t)$  values, which, together with Paleoproterozoic model ages, characterize Carboniferous Almansor and Valverde granitic rocks, indicate the involvement of ancient crustal material. The Cadomian basement is the most likely source of this because juvenile arc magmas associated with Neoproterozoic magmatic arc activity were contaminated by the Eburnian crust of the West African craton [76]. In turn, other samples of Almansor and Valverde granitic rocks and migmatites follow the flat trend of less LREE-enriched ca. 337 Ma Hospitais quartz dioritic rocks displaying negative  $\epsilon\text{Nd}(t)$  values from  $-1.9$  to  $-3.2$  [25] (Figure 9) and Nd model ages ranging from 1219 to 1769 Ma (Figure 8). Hospitais quartz diorites probably derived from parental mafic magmas formed in a metasomatized mantle wedge above a long-lived subduction zone or the mixing of mafic melts from a depleted mantle source and anatexis melts derived from Cambrian felsic metaigneous sources [25]. Conversely, Beja-Acebuches amphibolites of the same age present positive  $\epsilon\text{Nd}(t)$  values from  $+8.0$  to  $+9.2$  [60] and geologically unexpected model ages, which are significantly younger than their Carboniferous crystallization ages (Figure 8), indicative of a juvenile mantle source highly depleted in LREE. In contrast with this evidence of mantle rejuvenation, other samples of Beja-Acebuches amphibolites show negative  $\epsilon\text{Nd}(t)$  values from  $-2.2$  to  $-2.9$  and old Nd model ages (Figure 8) characteristic of a more greatly enriched mantle source consistent with some crustal contribution [23]. The emplacement of Visean plutonism was coeval, with flexural subsidence of continental lithosphere, marine sedimentation, and volcanism (ca. 335–331 Ma, Toca da Moura and Cabrela volcano-sedimentary complexes [16]) (Figure 9). Visean Toca da Moura bimodal volcanic rocks (Group 1), intercalated in turbidites, are interpreted as being genetically related to the fractional crystallization of parental magmas with a calc-alkaline composition, similar to taking place in recent magmatic arcs [50].

It is notable that the Nd isotopic signature of the more greatly enriched Toca da Moura rhyolitic rocks matches those of the Hospitais quartz diorites and gabbros with the youngest Nd model ages (Figure 8). This similarity suggests a link between magma chambers and volcanism. The other samples of the Toca da Moura rhyolites and trachyandesite show a trend marked by positive  $\epsilon\text{Nd}(t)$  values from  $+1.1$  to  $+1.9$  and younger Nd model ages of 782 to 1009 Ma, that is, close to the isotopic composition of the SCLM beneath the OMZ (Figure 8b). The variability recorded in Visean magmatic rocks from juvenile to enriched Nd isotopic compositions suggests the involvement of mantle sources and distinct degrees of crustal contribution.

Serpukhovian sedimentary and volcanic rocks are unknown in the OMZ. However, Serpukhovian plutonism is well represented in the Évora gneiss dome [25,26,33,34] (Figure 9).

The Serpukhovian plutonic rocks of Alto de São Bento and Pavia probably derived from magmatic differentiation and the melting of calc-alkaline magmatic and sedimentary



protoliths [18,24,27]. The granitic rocks of the Pavia pluton (ca. 328 Ma [26]) with positive  $\epsilon\text{Nd}(t) = +0.3$  to  $+3.0$  and negative  $\epsilon\text{Nd}(t) = -0.3$  to  $-2.7$  corresponding to  $T_{\text{DM}}$  ages of 821–871 Ma and 868–1068 Ma, respectively, are isotopically similar [27] (Figure 8). Less enriched granitic rocks fall into the range defined for the SCML beneath the OMZ. The other more enriched Pavia granitic rocks characterized by a pronounced negative Nb anomaly [27] follow a trend of isotopic composition, indicating contribution from crustal materials. Most Pavia pluton granitic rocks are chemically similar to adakites [27], suggesting derivation from the partial melting of a subducted oceanic lithosphere. In turn, Alto de São Bento orthomigmatites (metadioritic rocks) with Visean protolith age (ca. 338–336 Ma) contain granitic new melts (ca. 329–327 Ma; leucosomes) that are characterized by a typical arc calc-alkaline signature associated with a source of andesitic composition [18]. This finding supports the recycling of intermediate-mafic plutonic rocks, representing former stages of growth of the root of a magmatic arc at the time of the coeval subduction of the Paleotethys oceanic lithosphere [77].

The huge volume of Visean-Serpukhovian plutonic and volcanic rocks extending from the Évora gneiss dome and the Beja Igneous Complex to other eastern domains of the OMZ (Spain) (Figure 9) is regarded as representing the main stage of arc-derived magmatism in the Carboniferous [18,33,44] (Figure 10c).

#### 4.3. Bashkirian-Gzhelian: Latest Stage of Arc-Magmatism

Évora gneiss dome high-grade metamorphic rocks and the Visean Toca da Moura volcano-sedimentary complex are intruded by ca. 318 Ma Baleizão porphyries [16], interpreted as being a subvolcanic suite [45], which occupies an extensive area of the Beja Igneous Complex (Figure 9). Baleizão porphyries and Alcáçovas dioritic rocks ( $317 \pm 3$  Ma; this study) show significant enrichment in LREE and a more pronounced negative Eu anomaly as silica content increases. The fractionation of amphibole in intermediate magmas could be the cause of the mitigation of the negative Eu anomaly in Bashkirian quartz dioritic rocks, whereas the rhyolitic-to-dacitic composition of Baleizão porphyries is probably due to varying degrees of plagioclase fractionation [20]. Baleizão porphyries most likely crystallized from melts derived from the same parental magma that generated Alcáçovas intermediate rocks during the functioning of a subduction zone [20]. The Baleizão porphyries trend linking the ranges defined for the SCML beneath the OMZ and Ediacaran Série Negra metasedimentary rocks and Cambrian Early Rift Event rhyolitic rocks (Figure 8b) indicates either a more depleted mantle source ( $\epsilon\text{Nd}(t) = +3.7$  and  $T_{\text{DM}}$  age = 782 Ma) and more greatly enriched sources or a contaminated mantle-derived magma (negative  $\epsilon\text{Nd}(t) = -0.6$  to  $-1.7$  and older isotopic ages ranging from 1047 to 1153 Ma). The isotopic signature of Alcáçovas quartz diorite ( $\epsilon\text{Nd}(t)$  value =  $+3.8$  and TDM age = 782 Ma) is juvenile in comparison with Baleizão porphyries and similar to the more greatly depleted magmatic rocks of the Tournaisian Layered Gabbroic Sequence and the Serpukhovian Pavia pluton (Figure 8b), suggesting that they derived from the same mantle source and emplaced during the successive stages of arc magmatism.

The stratigraphy of the Serpukhovian marks a regional uplift event that probably coincides with the beginning of  $D_3$  contractional deformation in the OMZ (Figure 9a), as indicated by the evolution of the Carboniferous Guadalquivir basin, located near the boundary with the Central Iberian Zone ([78] Figure 9b). Later, the Moscovian to Gzhelian sedimentary record is characterized by continental sedimentation as a result of OMZ progressive uplift, mainly determined by active strike-slip faults [79]. Moscovian-Gzhelian volcanism is lacking in the stratigraphy but calc-alkaline plutonism is recognized in the Évora gneiss dome due to the presence of porphyritic granites (ca. 314–313 Ma [18,26,34]) (Figure 9). This plutonism extends further north, close to the boundary with the Central Iberian Zone, involving several plutons composed of granites and gabbro-dioritic rocks (ca. 303–297 Ma, Santa Eulália-Monforte massif [71]; and the Nisa-Albuquerque and Los Pedroches batholiths (ca. 314–303 Ma [72,73]) (Figures 1 and 8).

Moscovian-Gzhelian granitic and gabbro-dioritic rocks have geochemical signatures that are broadly similar to the Sierra Nevada and Patagonia batholiths of the North American Cordillera and the Andes continental active margins [71]. The gabbro-dioritic rocks forming the Santa Eulália-Monforte pluton yield  $\epsilon\text{Nd}(t)$  values from  $-2.9$  to  $+1.8$  and  $T_{\text{DM}}$  ages ranging from 995 to 1712 Ma, whereas granitic rocks from the same ca. 303 Ma pluton and the ca. 312 Ma Los Pedroches batholith present  $\epsilon\text{Nd}(t)$  values ranging from  $-0.8$  to  $-5.8$  corresponding to  $T_{\text{DM}}$  age = 938–1297 Ma (Figure 8). This evolutionary trend in terms of Nd isotopic composition coincides with those of Visean Toca da Moura volcanic rocks, Serpukhovian Pavia granitic rocks and Bashkirian Baleizão Porphyries (Figure 8b), suggesting a mixture of old crustal sources and less enriched sources derived from the SCLM beneath the OMZ or other juvenile mantle sources. This mixture of distinct components may have intensified in the main and latest stages of arc magmatism. The result of the simultaneous action of two major tectonic processes in the core of Pangea, including (i) the development of the Iberian oroclinal from the Moscovian to the Gzhelian [80] and (ii) the gradual northward drift of Cimmerian terranes toward the Eurasian active margin [81], may have favored the lateral migration of Paleotethys subduction and the associated magmatic arc during the Permian [82], leading to the waning of the evolution of the Paleotethys magmatic arc in southwestern Iberia (Figure 10d).

## 5. Conclusions

- (1) The enriched, continental-crust-like major and trace element features of the Carboniferous igneous rocks of the Beja Igneous Complex (Group 1—Toca da Moura and Group 2—Baleizão and Alcáçovas) and the Évora gneiss dome document three stages of arc magmatism, mainly with the addition of calc-alkaline magma extracted from various mantle sources, in a subduction-related setting (i.e., Paleotethys subduction).
- (2) The U-Pb zircon dating of  $317 \pm 3$  Ma confirms the Bashkirian age of Alcáçovas Qz-dioritic rock, which together with Baleizão porphyries, represents the latest stage of Carboniferous arc magmatism in the OMZ.
- (3) Positive  $\epsilon\text{Nd}(t)$  values for the Tournaisian-Bashkirian igneous rocks of the Beja Igneous Complex and the Évora gneiss dome indicate that the OMZ basement was a site of new juvenile crustal production in the Carboniferous. Furthermore, negative  $\epsilon\text{Nd}(t)$  values also suggest different grades of crustal contamination for this magmatism.
- (4) The Tournaisian-Bashkirian igneous rocks of the Beja Igneous Complex and Évora gneiss dome igneous rocks probably derived from a mantle-derived magma that interplayed, at different grades, with crustal-derived magmas. An active continental margin involving juvenile materials and crustal contamination is inferred for the tectonic setting, which determined the production and evolution of Carboniferous OMZ igneous rocks.
- (5) Our findings contribute to reinforcing the recently proposed tectonic model for this region of the Iberian Variscan belt. It is reasonable that subduction of Paleotethys oceanic lithosphere under the OMZ, close to a former (Rheic Ocean) suture zone, was contemporaneous with collisional orogenic processes. This tectonic framework may explain the Carboniferous spatial distribution of crustal extension, dome formation, exhumation of high-grade metamorphic rocks, and compositional variations of syn-orogenic magmatism dominated by arc-like signatures that lasted for at least 60 m.y. in this region of the Pangea supercontinent.

**Supplementary Materials:** The following supporting information can be downloaded at: <https://www.mdpi.com/article/10.3390/min12050597/s1>. Table S1: Whole-rock geochemistry (major and trace elements): Toca da Moura (TM) rhyolites and trachyandesite, Baleizão (BL) porphyries and Alcáçovas (ALC) quartz dioritic rock; Table S2: Sm-Nd isotopes: Toca da Moura (TM) rhyolites and trachyandesite, Baleizão (BL) porphyries and Alcáçovas (ALC) quartz dioritic rock; Table S3: U-Pb zircon geochronology: Alcáçovas quartz dioritic rock; Text S4: Analytical Methods.

**Author Contributions:** Conceptualization, M.F.P.; methodology, M.F.P.; investigation, M.F.P., J.M.F., C.R. and A.C.; resources, M.F.P. and A.C.; writing—original draft preparation, M.F.P. and C.R.; writing—review and editing, M.F.P., J.M.F., C.R. and A.C.; supervision, M.F.P.; funding acquisition, M.F.P. and A.C. All authors have read and agreed to the published version of the manuscript.

**Funding:** This work was supported by the financial support of the Portuguese Foundation for Science and Technology project UIDB-04683-2020-ICT and by the Spanish Research Agency, grant PGC2018-096534-B-I00 IBERCRUST.

**Data Availability Statement:** Not applicable.

**Acknowledgments:** The authors are grateful for technical and human support provided by SGiker of UPV-EHU and European funding (ERDF and ESF). This is a IBERSIMS publication no.99. This paper is a contribution to project IUGS-UNESCO IGCP 683, Pre-Atlantic geological connections among northwest Africa, Iberia and eastern North America: implications for continental configurations and economic resources.

**Conflicts of Interest:** The authors declare no conflict of interest.

## References

1. Cawood, P.A.; Hawkesworth, C.J.; Dhuime, B. The continental record and the generation of continental crust. *GSA Bull.* **2013**, *125*, 14–32. [[CrossRef](#)]
2. Frost, B.R.; Barnes, C.G.; Collins, W.J.; Arculus, R.J.; Ellis, D.J.; Frost, C.D. A geochemical classification for granitic rocks. *J. Petrol.* **2001**, *42*, 2033–2048. [[CrossRef](#)]
3. Rudnick, R.L.; Gao, S. Composition of the continental crust. In *Treatise on Geochemistry, The Crust*; Rudnick, R.L., Ed.; Elsevier: Amsterdam, The Netherlands, 2003; p. 64.
4. DePaolo, D.J. *Neodymium Isotope Geochemistry. An Introduction*; Minerals and Rocks Series 1988, No. 20; Springer: Berlin/Heidelberg, Germany, 1988; 187p.
5. Cawood, P.A.; Kröner, A.; Collins, W.J.; Kusky, T.M.; Mooney, W.D.; Windley, B.F. Accretionary orogens through Earth history. *Geol. Soc. Lond. Spec. Publ.* **2009**, *318*, 1–36. [[CrossRef](#)]
6. Scholl, D.W.; von Huene, R. Implications of estimated additions and recycling losses at the subduction zones of accretionary (non-collisional) and collisional (suturing) orogens. *Geol. Soc. Lond. Spec. Publ.* **2009**, *318*, 105–125. [[CrossRef](#)]
7. Tang, G.J.; Chung, S.L.; Hawkesworth, C.J.; Cawood, P.A.; Wang, Q.; Wyman, D.A.; Xu, Y.G.; Zhao, Z.H. Short episodes of crust generation during protracted accretionary processes: Evidence from Central Asian Orogenic Belt, NW China. *Earth Planet. Sci. Lett.* **2017**, *464*, 142–154. [[CrossRef](#)]
8. Dostal, J.; Murphy, J.B.; Shellnutt, J.G. Secular isotopic variation in lithospheric mantle through the Variscan orogen: Neoproterozoic to Cenozoic magmatism in continental Europe. *Geology* **2019**, *47*, 637–640. [[CrossRef](#)]
9. Benoit, M.; Aguillón-Borges, A.; Calmus, T.; Maury, R.C.; Bellon, H.; Cotton, J.; Bourgois, J.; Michaud, F. Geochemical Diversity of Late Miocene Volcanism in Southern Baja California, Mexico: Implication of Mantle and Crustal Sources during the Opening of an Asthenospheric Window. *J. Geol.* **2002**, *110*, 627–648. [[CrossRef](#)]
10. Simancas, J.F.; Tahiri, A.; Azor, A.; González Lodeiro, F.; Martínez Poyatos, D.; El Hadi, H. The tectonic frame of the Variscan-Alleghanian orogen in southern Europe and northern Africa. *Tectonophysics* **2005**, *398*, 181–198. [[CrossRef](#)]
11. Ribeiro, A.; Munhá, J.; Dias, R.; Mateus, A.; Pereira, E.; Ribeiro, L.; Fonseca, P.; Araújo, A.; Oliveira, T.; Romão, J.; et al. Geodynamic evolution of the SW Europe Variscides. *Tectonics* **2007**, *26*, TC6009. [[CrossRef](#)]
12. Braid, J.A.; Murphy, J.B.; Quesada, C.; Mortensen, J. Tectonic escape of a crustal fragment during the closure of the Rheic Ocean: U–Pb detrital zircon data from the late Palaeozoic Pulo de Lobo and South Portuguese Zones, Southern Iberia. *J. Geol. Soc.* **2011**, *168*, 383–392. [[CrossRef](#)]
13. Pérez-Cáceres, I.; Martínez Poyatos, D.; Simancas, J.F.; Azor, A. The elusive nature of the Rheic Ocean suture in SW Iberia. *Tectonics* **2015**, *34*, 2429–2450. [[CrossRef](#)]
14. Díez Fernández, R.; Arenas, R.; Pereira, M.F.; Sánchez Martínez, S.; Albert, R.; Martín Parra, L.M.; Rubio Pascual, F.J.; Matas, J. Tectonic evolution of Variscan Iberia: Gondwana-Laurussia collision revisited. *Earth-Sci. Rev.* **2016**, *162*, 269–292. [[CrossRef](#)]
15. Murphy, J.B.; Quesada, C.; Gutiérrez-Alonso, G.; Johnston, S.T.; Weil, A. Reconciling competing models for the tectono-stratigraphic zonation of the Variscan orogen in Western Europe. *Tectonophysics* **2016**, *681*, 209–219. [[CrossRef](#)]
16. Pereira, M.F.; Gama, C.; Dias da Silva, Í.; Silva, J.B.; Hofmann, M.; Linnemann, U.; Gärtner, A. Chronostratigraphic framework and provenance of the Ossa-Morena Zone Carboniferous basins (southwest Iberia). *Solid Earth* **2020**, *11*, 1291–1312. [[CrossRef](#)]
17. Pereira, M.F.; Gutiérrez-Alonso, G.; Murphy, J.B.; Drost, K.; Gama, C.; Silva, J.B. Birth and demise of the Rheic Ocean magmatic arc(s): Combined U–Pb and Hf isotope analyses in detrital zircon from SW Iberia siliciclastic strata. *Lithos* **2017**, *278*, 383–399. [[CrossRef](#)]
18. Rodríguez, C.; Pereira, M.F.; Castro, A.; Gutiérrez-Alonso, G.; Fernández, C. Variscan intracrustal recycling by melting of Carboniferous arc-like igneous protoliths (Évora Massif, Iberian Variscan belt). *GSA Bull.* **2022**, *134*, 1549–1570. [[CrossRef](#)]

19. Romeo, I.; Lunar, R.; Capote, R.; Quesada, C.; Dunning, G.R.; Pina, R.; Ortega, L. U-Pb age constraints on Variscan magmatism and Ni-Cu-PGE metallogeny in the Ossa-Morena Zone (SW Iberia). *J. Geol. Soc.* **2006**, *163*, 837–846. [[CrossRef](#)]
20. Caldeira, R.; Ribeiro, M.L.; Moreira, M.E. Geoquímica das sequências máficas e félsicas entre Alvito, Torrão e Alcáçovas (SW da ZOM). *Comun. Geológicas* **2007**, *94*, 5–28.
21. Jesus, A.; Munhá, J.; Mateus, A.; Tassinari, C.; Nutman, A. The Beja layered gabbroic sequence (Ossa-Morena Zone, Southern Portugal): Geochronology and geodynamic implications. *Geodin. Acta* **2007**, *20*, 139–157. [[CrossRef](#)]
22. Jesus, A.P.; Mateus, A.; Munhá, J.M.; Tassinari, C.G.; Bento dos Santos, T.M.; Benoit, M. Evidence for underplating in the genesis of the Variscan synorogenic Beja Layered Gabbroic Sequence (Portugal) and related mesocratic rocks. *Tectonophysics* **2016**, *683*, 148–171. [[CrossRef](#)]
23. Pin, C.; Fonseca, P.E.; Paquette, J.L.; Castro, P.; Matte, P. The ca. 350 Ma Beja igneous complex: A record of transcurrent slab break-off in the southern Iberia Variscan Belt? *Tectonophysics* **2008**, *461*, 356–377. [[CrossRef](#)]
24. Moita, P.; Santos, J.F.; Pereira, M.F. Layered granitoids: Interaction between continental crust recycling processes and mantle-derived magmatism: Examples from the Évora Massif (Ossa-Morena Zone, southwest Iberia, Portugal). *Lithos* **2009**, *111*, 125–141. [[CrossRef](#)]
25. Moita, P.; Santos, J.F.; Pereira, M.F.; Costa, M.M.; Corfu, F. The quartz dioritic Hospitais intrusion (SW Iberian Massif) and its mafic micro-granular enclaves- Evidence for mineral clustering. *Lithos* **2015**, *224*, 78–100. [[CrossRef](#)]
26. Lima, S.M.; Corfu, F.; Neiva, A.M.R.; Ramos, M.F. Dissecting complex magmatic processes: An in-depth U-Pb study of the Pavia Pluton, Ossa-Morena Zone, Portugal. *J. Petrol.* **2012**, *53*, 1887–1911. [[CrossRef](#)]
27. Lima, S.M.; Neiva, A.M.R.; Ramos, J.M.F. Adakitic-like magmatism in western Ossa-Morena Zone (Portugal): Geochemical and isotopic constraints of the Pavia pluton. *Lithos* **2013**, *160*, 98–116. [[CrossRef](#)]
28. Ferreira, P.; Caldeira, R. and Calvo, R. Geoquímica das rochas ígneas aflorantes na região de S. Matias, Cuba (Alentejo). *Comun. Geológicas* **2014**, *101*, 93–97.
29. Cambeses, A.; Scharrow, J.H.; Montero, P.; Molina, J.F.; Moreno, J.A. SHRIMP U-Pb zircon dating of the Valencia del Ventoso plutonic complex, Ossa-Morena Zone, SW Iberia: Early Carboniferous intra-orogenic extension-related ‘calc-alkaline’ magmatism. *Gondwana Res.* **2015**, *28*, 735–756. [[CrossRef](#)]
30. Carvalho, D.; Goinhas, J.; Oliveira, J.T.; Ribeiro, A. Observações sobre a geologia do Sul de Portugal e consequências metalogénicas. *Estudos, Notas e Trabalhos. Serviços Fom. Min.* **1971**, *20*, 153–199.
31. Barros, A.; Carvalhosa, A.B.; Zbyszewski, G. Carta Geológica de Portugal, scale 1:50 000. In *Notícia Explicativa da Folha 40-C: Viana do Alentejo*; Serviços Geológicos de Portugal: Lisboa, Portugal, 1972; p. 24.
32. Gonçalves, F.; Telles, A. Carta Geológica de Portugal, scale, 1/50 000. In *Notícia Explicativa da Folha 39-D Torrão*; Serviços Geológicos de Portugal: Lisboa, Portugal, 1992; 32p.
33. Oliveira, J.T.; Pereira, E.; Ramalho, M.; Antunes, M.T.; Monteiro, J.H. *Carta Geológica de Portugal, Scale 1/500.000*; Serviços Geológicos de Portugal: Lisboa, Portugal, 1992.
34. Pereira, M.F.; Chichorro, M.; Williams, I.S.; Silva, J.B.; Fernandez, C.; Diaz-Azpiroz, M.; Apraiz, A.; Castro, A. Variscan intra-orogenic extensional tectonics in the Ossa-Morena Zone (Évora-Aracena-Lora del Rio metamorphic belt, SW Iberian Massif): SHRIMP zircon U-Th-Pb geochronology. In *Ancient Orogens and Modern Analogues*; Murphy, J.B., Keppie, J.D., Hynes, A.J., Eds.; Geological Society of America: Boulder, CO, USA, 2009; Volume 327, pp. 215–237.
35. Dias da Silva, Í.; Pereira, M.F.; Silva, J.B.; Gama, C. Time-space distribution of silicic plutonism in a gneiss dome of the Iberian Variscan Belt: The Évora Massif (Ossa-Morena Zone, Portugal). *Tectonophysics* **2018**, *747*, 298–317. [[CrossRef](#)]
36. Pereira, M.F.; Chichorro, M.; Williams, I.S.; Silva, J.B. Zircon U-Pb geochronology of paragneisses and biotite granites from the SW Iberia Massif. (Portugal): Evidence for a paleogeographic link between the Ossa-Morena Ediacaran basins and the West African craton. In *The Boundaries of the West African Craton*; Ennih, N., Liégeois, J.P., Eds.; Geological Society of America: Boulder, CO, USA, 2008; Volume 297, pp. 385–408.
37. Díez-Fernández, R.D.; Fuenlabrada, J.M.; Chichorro, M.; Pereira, M.F.; Sánchez-Martínez, S.; Silva, J.B.; Arenas, R. Geochemistry and tectonostratigraphy of the basal allochthonous units of SW Iberia (Évora Massif, Portugal): Keys to the reconstruction of pre-Pangean paleogeography in southern Europe. *Lithos* **2017**, *268*, 285–301. [[CrossRef](#)]
38. Chichorro, M.; Pereira, M.F.; Díaz-Azpiroz, M.; Williams, I.S.; Fernández, C.; Pin, C.; Silva, J.B. Cambrian ensialic rift-related magmatism in the Ossa-Morena Zone (Évora-Aracena metamorphic belt, SW Iberian Massif): Sm-Nd isotopes and SHRIMP zircon U-Th-Pb geochronology. *Tectonophysics* **2008**, *461*, 91–113. [[CrossRef](#)]
39. Pereira, M.F.; Silva, J.B.; Chichorro, M.; Moita, P.; Santos, J.F.; Apraiz, A.; Ribeiro, C. Crustal growth and deformational processes in the Northern Gondwana margin: Constraints from the Évora Massif (Ossa-Morena Zone, SW Iberia, Portugal). In *The Evolution of the Rheic Ocean: From Avalonian-Cadomian Active Margin to Alleghenian-Variscan Collision*; Linnemann, U., Nance, R.D., Kraft, P., Zulauf, G., Eds.; Geological Society of America: Boulder, CO, USA, 2007; Volume 423, pp. 333–358.
40. Sánchez-García, T.; Bellido, F.; Pereira, M.F.; Chichorro, M.; Quesada, C.; Pin, C.; Silva, J.B. Rift related volcanism predating the birth of the Rheic Ocean (Ossa-Morena Zone, SW Iberia). *Gondwana Res.* **2010**, *17*, 392–407. [[CrossRef](#)]
41. Díez Fernández, R.; Pereira, M.F.; Foster, D.A. Peralkaline and alkaline magmatism of the Ossa-Morena zone (SW Iberia): Age, source, and implications for the Paleozoic evolution of Gondwanan lithosphere. *Lithosphere* **2015**, *7*, 73–92. [[CrossRef](#)]

42. Rojo-Pérez, E.; Fuenlabrada, J.M.; Linnemann, U.; Arenas, R.; Sánchez Martínez, S.; Díez Fernández, R.; Martín Parra, L.M.; Matas, J.; Andonaegui, P.; Fernández-Suárez, J. Geochemistry and Sm-Nd isotopic sources of Late Ediacaran siliciclastic series in the Ossa-Morena Complex: Iberian-Bohemian correlations. *Int. J. Earth Sci.* **2021**, *110*, 467–485. [[CrossRef](#)]
43. Pereira, M.F.; Chichorro, M.; Silva, J.; Ordóñez-Casado, B.; Lee, J.; Williams, I. Early Carboniferous wrenching, exhumation of high-grade metamorphic rocks and basin instability in SW Iberia; constrains derived from structural geology and U–Pb and  $^{40}\text{Ar}$ – $^{39}\text{Ar}$  geochronology. *Tectonophysics* **2012**, *558*, 28–44. [[CrossRef](#)]
44. Pereira, M.F.; Chichorro, M.; Moita, P.; Santos, J.F.; Solá, A.M.R.; Williams, I.S.; Silva, J.B.; Armstrong, R.A. The multistage crystallization of zircon in calc-alkaline granitoids: U–Pb age constraints on the timing of Variscan tectonic activity in SW Iberia. *Int. J. Earth Sci.* **2015**, *104*, 1167–1183. [[CrossRef](#)]
45. Gonçalves, F.; Carvalhosa, A. Subsídios para o conhecimento geológico do Carbónico de Santa Susana Vol. D' Hommage au géologue G. Zbyszewski. *Rech. Civilis.* **1984**, *109*, 136.
46. Santos, J.F.; Andrade, A.S.; Munhá, J. Magmatismo orogénico Varisco no limite meridional da Zona de Ossa-Morena. *Comun. Serviços Geológicos Port.* **1990**, *76*, 91–124.
47. Domingos, L.C.G.; Freire, J.L.S.; Silva, F.G.; Gonçalves, F.; Pereira, E.; Ribeiro, A. The Structure of the Intramontane Upper Carboniferous Basins in Portugal. In *The Carboniferous of Portugal. Memórias, Nova Série 29*; de Sousa, M.J.L., Oliveira, J.T., Eds.; Serviços Geológicos de Portugal: Lisboa, Portugal, 1983; pp. 187–194.
48. Machado, G.; Dias da Silva, I.; Almeida, P. Palynology, stratigraphy and geometry of the Pennsylvanian continental Santa Susana Basin (SW Portugal). *J. Iber. Geol.* **2012**, *38*, 429–448.
49. Dinis, P.A.; Fernandes, P.; Jorge, R.S.; Rodrigues, B.; Chew, D.M.; Tassinari, C. The transition from Pangea amalgamation to fragmentation: Constraints from detrital zircon geochronology on West Iberia paleogeography and sediment sources. *Sediment. Geol.* **2018**, *375*, 172–187. [[CrossRef](#)]
50. Santos, J.; Mata, J.; Gonçalves, F.; Munhá, J. Contribuição para o conhecimento Geológico-Petrológico da Região de Santa Susana: O Complexo Vulcano-sedimentar da Toca da Moura. *Comun. dos Serviços Geológicos Port.* **1987**, *73*, 29–48.
51. Pearce, J.A. The role of the sub-continental lithosphere in magma genesis at destructive plate margins. In *Continental Basalts and Mantle Xenoliths*; Hawkesworth, C.J., Norry, M.J., Eds.; Shiva Publications: Nantwich, UK, 1983; pp. 230–249.
52. Pearce, J.A.; Harris, N.; Tindle, A.G. Trace element discrimination diagrams for the tectonic interpretation of granitic rocks. *J. Petrol.* **1984**, *25*, 956–983. [[CrossRef](#)]
53. Díez Fernández, R.; Pereira, M.F. Extensional orogenic collapse captured by strike-slip tectonics: Constraints from structural-geology and U–Pb geochronology of the Pinhel shear zone (Variscan orogen, Iberian Massif). *Tectonophysics* **2016**, *691*, 290–310. [[CrossRef](#)]
54. Pereira, M.F.; Díez Fernández, R.; Gama, C.; Hofmann, M.; Gartner, A.; Linnemann, U. S-type granite generation and emplacement during a regional switch from extensional to contractional deformation (Central Iberian Zone, Iberian autochthonous domain, Variscan Orogeny). *Int. J. Earth Sci.* **2018**, *107*, 251–267. [[CrossRef](#)]
55. Dias da Silva, Í.; González Clavijo, E.; Díez-Montes, A. The collapse of the Variscan belt: A Variscan lateral extrusion thin-skinned structure in NW Iberia. *Int. Geol. Rev.* **2020**, *63*, 659–695. [[CrossRef](#)]
56. Fernández-Suárez, J.; Dunning, G.R.; Jenner, G.A.; Gutiérrez-Alonso, G. Variscan collisional magmatism and deformation in NW Iberia: Constraints from U–Pb geochronology of granitoids. *J. Geol. Soc.* **2000**, *157*, 565–576. [[CrossRef](#)]
57. Gutiérrez-Alonso, G.; Fernández-Suárez, J.; Jeffries, T.E.; Johnston, S.T.; Pastor-Galán, D.; Murphy, J.B.; Piedad Franco, M.; Gonzalo, J.C. Diachronous post-orogenic magmatism within a developing orocline in Iberia, European Variscides. *Tectonics* **2011**, *30*, TC5008. [[CrossRef](#)]
58. Castro, A.; Gerya, T.V.; García-Casco, A.; Fernandez, C. Melting Relations of MORB-Sediment Melanges in Underplated Mantle Wedge Plumes; Implications for the Origin of Cordilleran-type Batholiths. *J. Petrol.* **2010**, *51*, 1267–1295. [[CrossRef](#)]
59. Gutiérrez-Alonso, G.; Murphy, J.B.; Fernández-Suárez, J.; Weil, A.B.; Franco, M.P.; Gonzalo, J.C. Lithospheric delamination in the core of Pangea: Sm–Nd insights from the Iberian mantle. *Geology* **2011**, *39*, 155–158. [[CrossRef](#)]
60. Castro, A.; Fernández, C.; de la Rosa, J.D.; Moreno-Ventas, I.; El Hmidi, H.; El Biad, M.; Bergamin, J.F.; Sánchez, N. Triple-junction migration during Paleozoic Plate convergence: The Aracena metamorphic belt, Hercynian massif, Spain. *Geol. Rundsch.* **1996**, *85*, 108–185. [[CrossRef](#)]
61. Pin, C.; Liñan, E.; Pascual, E.; Donaire, T.; Velenzuela, A. Late Neoproterozoic crustal growth in the European Variscides: Nd isotope and geochemical evidence from the Sierra de Córdoba Andesites (Ossa-Morena Zone, Southern Spain). *Tectonophysics* **2002**, *352*, 133–1581. [[CrossRef](#)]
62. Lopes, J.M.C. Petrologia e Geoquímica de Complexos Plutónicos do NE Alentejano (Z.O.M.), Portugal central—Província Alcalina e Maciço de Campo Maior. Ph.D. Thesis, Universidade de Évora, Évora, Portugal, 2004; p. 505, (Unpublished).
63. Puziewicz, J.; Matusiak-Malek, M.; Ntaflos, T.; Grégoire, M.; Kaczmarek, M.A.; Aulbach, S.; Ziobro, M.; Kukula, A. Three major types of subcontinental mantle beneath the Variscan orogeny in Europe. *Lithos* **2020**, *362–363*, 105467. [[CrossRef](#)]
64. Villaseca, C.; Orejana, D.; Higuera, P.; Pérez-Soba, C.; García Serrano, J.; Lorenzo, S. The evolution of the subcontinental mantle beneath the Central Iberian Zone: Geochemical tracking of its mafic magmatism from the Neoproterozoic to the Cenozoic. *Earth-Sci. Rev.* **2022**, *228*, 103997. [[CrossRef](#)]
65. Quesada, C.; Robardet, M.; Gabaldon, V. Ossa-Morena Zone. Stratigraphy. Synorogenic phase (Upper Devonian–Carboniferous–Lower Permian). *Pre-Mesoz. Geol. Iber.* **1990**, *273–279*.

66. Armendáriz, M.; López-Guijarro, R.; Quesada, C.; Pin, C.; Bellido, F. Genesis and evolution of a syn-orogenic basin in transpression: Insights from petrography, geochemistry and Sm-Nd systematics in the Variscan Pedroches basin (Mississippian, SW Iberia). *Tectonophysics* **2008**, *461*, 395–413. [[CrossRef](#)]
67. Casquet, C.; Galindo, C.; Darbyshire, D.P.F.; Noble, S.R.; Tornos, F. Fe-U-REE mineralization at Mina Monchi, Burguillos del Cerro, SW Spain. Age and isotope (U-Pb, Rb-Sr, Sm-Nd) constraints on the evolution of the ores. In Proceedings of the GAC-MAC-APGGQ Quebec '98 Conference, Quebec, QC, Canada, 18–20 May 1998; Abstract Volume 23: A-28.
68. Montero, P.; Salman, K.; Bea, F.; Azor, A.; Exposito, I.; González-Lodeiro, F.; Martínez Poyatos, D.J.; Simancas, J.F. New data on the geochronology of the Ossa Morena Zone, Iberian Massif. *Basement Tecton.* **2000**, *15*, 136–138.
69. Antunes, A.; Santos, J.F.; Azevedo, M.R.; Corfu, F. New U-Pb zircon age constraints for the emplacement of the Reguengos de Monsaraz Massif (Ossa Morena Zone). In *Seventh Hutton Symposium on Granites and Related Rocks-Abstracts Book, Proceedings of VII Hutton Symposium on Granites and Related Rocks, Avila, Spain, 4–9 July 2011*; Elsevier: Amsterdam, The Netherlands, 2011; pp. 9–10.
70. Azor, A.; Rubatto, D.; Simancas, J.F.; González Lodeiro, F.; Martínez Poyatos, D.; Martín Parra, L.M.; Matas, J. Rheic Ocean ophiolitic remnants in southern Iberia questioned by SHRIMP U-Pb zircon ages on the Beja-Acebuches amphibolites. *Tectonics* **2008**, *27*, TC5006. [[CrossRef](#)]
71. Pereira, M.F.; Gama, C.; Rodríguez, C. Coeval interaction between magmas of contrasting composition (Late Carboniferous-Early Permian Santa Eulália-Monforte massif, Ossa-Morena Zone): Field relationships and geochronological constraints. *Geol. Acta* **2017**, *15*, 409–428.
72. Solá, A.R.; Williams, I.S.; Neiva, A.M.R.; Ribeiro, M.L. U-Th-Pb SHRIMP ages and oxygen isotope composition of zircon from two contrasting late Variscan granitoids, Nisa- Albuquerque batholith, SW Iberian Massif: Petrologic and regional implications. *Lithos* **2009**, *111*, 156–167. [[CrossRef](#)]
73. Carracedo, M.; Paquette, J.L.; Alonso Olazabal, A.; Santos Zalduegui, J.F.; García de Madinabeitia, S.; Tiepolo, M.; Gil Iburguchi, J.I. U-Pb dating of granodiorite and granite units of the Los Pedroches batholith. Implications for geodynamic models of the southern Central Iberian Zone (Iberian Massif). *Int. J. Earth Sci.* **2008**, *98*, 1659. [[CrossRef](#)]
74. Ordóñez-Casado, B.; Martín-Izard, A.; García-Nieto, J. SHRIMP-zircon U-Pb dating of the Ni-Cu-PGE mineralized Aguablanca gabbro and Santa Olalla granodiorite: Confirmation of an Early Carboniferous metallogenic epoch in the Variscan Massif of the Iberian Peninsula. *Ore Geol. Rev.* **2008**, *34*, 343–353. [[CrossRef](#)]
75. Quesada, C.; Fonseca, P.E.; Munha, J.; Oliveira, J.T.; Ribeiro, A. The Beja-Acebuches Ophiolite (Southern Iberia Variscan fold belt): Geological characterization and significance. *Bol. Geológico Min.* **1994**, *105*, 3–49.
76. Linnemann, U.; Gerdes, A.; Hofmann, M.; Marko, L. The Cadomian Orogen: Neoproterozoic to Early Cambrian crustal growth and orogenic zoning along the periphery of the West African Craton- Constraints from U-Pb zircon ages and Hf isotopes (Schwarzburg Antiform, Germany). *Precambrian Res.* **2014**, *244*, 236–278. [[CrossRef](#)]
77. Martín-Catalán, J.R.; Schulmann, K.; Ghienne, J.F. The Mid-Variscan Allochthon: Keys from correlation, partial retrodeformation and plate-tectonic reconstruction to unlock the geometry of a non-cylindrical belt. *Earth-Sci. Rev.* **2021**, *220*, 103700. [[CrossRef](#)]
78. Matas, J.; Martín Parra, L.M.; Santiago, M.M. Un olistostroma con cantos y bloques del Paleozoico inferior en la Cuenca Carbonífera del Guadalquivir (Córdoba). Parte I: Estratigrafía y marco geodinámico Varisco. *Rev. Soc. Geol. España* **2014**, *27*, 11–25.
79. Wagner, R.H. The Iberian Massif: A Carboniferous assembly. *J. Iber. Geol.* **2004**, *30*, 93–108.
80. Gutiérrez-Alonso, G.; Fernández-Suárez, J.; Weil, A.B. Orocline-triggered lithospheric delamination. In *Orogenic Curvature: Integrating Paleomagnetic and Structural Analyses*; Sussman, A.J., Weil, A.B., Eds.; Geological Society of America: Boulder, CO, USA, 2004; Volume 383, pp. 121–130.
81. Stampfli, G.M.; Kozur, H.W. Europe from the Variscan to the Alpine Cycles. In *European Lithosphere Dynamics*; Gee, D.G., Stephenson, R.A., Eds.; Geological Society of London Memoirs: Bath, UK, 2006; Volume 32, pp. 57–82.
82. Pereira, M.F.; Castro, A.; Fernández, C. The inception of a Paleotethyan magmatic arc in Iberia. *Geosci. Front.* **2015**, *6*, 297–306. [[CrossRef](#)]